BioCore
Exploring Scientific Community

International Journal of Nanotechnology in Medicine & Engineering

Research Article
ISSN 2474-8811

Strange Effect of a Synthesized Nanopackage Towards A549, Huh-7, A-375, KB44, MCF-7 And HT29 Human Cancer Therapy

Zahra Fakhroueian[1], Pouriya Esmaeilzadeh[2], Seyed-Behnam Ghaffari[3], Pegah Esmaeilzadeh[4]

[1]*School of Chemical Engineering-Nanomedicine, College of Engineering, Institute of Petroleum Engineering (IPE), University of Tehran, Iran.*
[2]*School of Chemical Engineering, Iran University of Science and Technology (IUST), Narmak, Tehran 16765-163, Iran.*
[3]*School of Chemical Engineering-Nanomaterials, College of Engineering, University of Tehran, Tehran, Iran.*
[4]*Institute of Pharmacy, Martin Luther University Halle-Wittenberg, 06120 Halle (Saale), Germany.*

Abstract

In this research, an unrivaled water-based eco-friendly nanopackage was designed including ZnO@modified-CNTs, alumina@silica, ZnO quantum dot NPs, pharmaceutical binder, viscosity control, emulsifier and dispersing agents. Characterizing the final nanofluid, the SEM, FTIR, XRD and UV-Vis were applied. The inhibition of cell growth for this nanopackage was evaluated by MTT assay against A549, Huh-7, A-375, KB44, MCF-7, and HT29 cell lines after incubation period of 24 and 48 h. Interestingly, the nanopackage treatments during 48 h showed no toxicity against normal human foreskin fibroblast cells (HFF-2) as a control. The obtained values of IC50 (µg/ml) were determined as follow: A549 cells (60), Huh-7 cells (75), A-375 cells (90), KB44 cells (65), MCF-7 cells (50), and HT29 cells (75) after 48 h of exposure with comparison of 195 (µg/ml) for control, respectively ($P<0.05$). The nanoproduct indicated very potential as selective and smart cytotoxic agent for inhibiting the growth, proliferation and eradication of these current cancer cells. Strong diffusion, smart surface modification, structural defects and ROS process can possess extravagant roles in oxidation-reduction chemical reactions related to cancer therapy and kinds of virus infections.

Keywords: ZnO quantum dot NPs, ZnO@ modified-CNTs, Surface hydrophilic functionalization, Smart nanodrug, Cancer therapy, Nanopackage, Anti-virus, Redox reaction, Biological system.

Corresponding author: Zahra Fakhroueian

School of Chemical Engineering-Nanomedicine, College of Engineering, Institute of Petroleum Engineering (IPE), University of Tehran, Iran.
E-mail: fakhroueian@ut.ac.ir

Citation: Zahra Fakhroueian *et.al.*(2020), Strange effect of a synthesized nanopackage towards A549, Huh-7, A-375, KB44, MCF-7 and HT29 human cancer therapy . Int J Nano Med & Eng. 5:4,

Received: August 05, 2020
Accepted: August 24, 2020
Published: October 20, 2020

Introduction

Cancer is a multiple chronic, complex and primordial disease, being still one of the most difficult healthcare problems in the world right now, which is projected to increase with an estimated 12 million deaths in 2030 [1-3]. Current treatments may include radiation, chemotherapy, immune therapy, phototherapy and surgery [4-7] but the effects of these various procedures may harm healthy cells/tissues, and induce local toxicity and embolism [8-11]. In recent years, nanotechnology science has emerged, being raised from fundamental physics, chemistry, biology and technology of nanometer scales. It has, therefore, been able to help all the knowledges in the world, as such anti-cancer drug designs in the form of advanced nanomedicine methods [12-17]. Therewith, metal oxide NPs showed superior efficacy and specified enhanced cytotoxicity, and are promising anticancer agents such as Ag, TiO_2, SiO_2, MgO, Al_2O_3, Fe_3O_4, CeO_2, ZrO_2, CrO_2, CuO, ZnO, carbon nanotubes (CNTs), and also their mixed oxides and nanocomposites [17-20].

Towards selection of progressive ideas, the effect of zinc oxide and aluminum oxide NPs was studied together in 2019 by Subramaniam et al. [21] for human HT29 colon cancer cell lines. The results describe that ZnO NPs are found to be more effective than alumina NPs in reducing in human HT29 colon cancer cell line proliferation, having much enhanced potentials and capabilities. Studies reported for human lung epithelial cells (L-132) and human alveolar adenocarcinoma cell line A549 were also showed that ZnO NPs can selectively diffuse into tumor cells, and thereby, interact

with the cancerous cells and surpass them through oxidative stress reactions and lipid peroxidations [21]. Noteworthy, ZnO NPs and their authoritative hydrophilic surface-modified derivatives and functionalizing them with antibodies revealed that they could preferentially kill various cancer cells with strikingly being less toxic against normal cells [18]. Then, the surface modification science of nanoplatforms opened our mind to much newer knowledge on this problem [22,23]. ZnO NPs and their authoritative hydrophilic surface-modified derivatives were considered to be a generally recognized as safe material by the FDA. ZnO NPs and their very efficient derivatives groups such as ZnO quantum dot NPs (Q-Dot NPs), are environmentally friendly and active inorganic amphoteric semiconductors. They also have unique properties such as good biocompatibility, strong surface energy, aqueous solubility, stability, enhanced permeability and high smart selectivity [1,18]. The Q-Dot NPs possess a larger percentage of atoms at their surfaces with quantum effects, which can lead to increased surface reactivity. They can load with the therapeutic drugs for superior delivering to target cells, and deeply diffuse into tumor sites and cancerous cells [22]. Q-Dot NPs influence drug loading, drug release and stability of the therapeutic agents because of their particular ultrasmall size (1-8 nm) and highly discrete and quantized electronic levels in individual transition states. Such small nanometer-sized and grate mobility, equip them with notable qualities that are not found in the same nanomaterial at larger size [17]. In particular, the fine ZnO Q-Dots NPs form nanocrystals include interstitial zinc ion (Zn+2) and, high trapping states, and oxygen vacancies, then, such type of nanocrystal generates many specific defect effects and electron attractions which can lead to a large number of electron-hole pairs (e^- h^+) complex. These positive holes (h^+) are very strong oxidative agents and can split water molecules derived from the ZnO NPs in aqueous medium, and run chemical reactions with cytoplasmic membrane at the interface state.

To get sufficient clinical predictive power, we explore the evidence of 6 cancer cell line models. As lead ideas on the subject, tetrapod-like ZnO nanocomposites in A375 cells studies (a human melanoma cell line) [24-26], Al2O3 NPs in human prostate cancer cells with strong antimicrobial activities [27], SiO2 NPs for treatment of the most common cancers in women, that is MCF-7 breast cancer [14,28], SiO2 NPs in HeLa human cervix cancer cells [29], nanographene oxide (NGO) NPs as an NGO-PEG-PEI/Cer formation (Ceramide-Graphene Oxide nanoparticles) in Hepatocellular carcinoma (HCC) [30,31], and ZnO Q-Dot semiconductor nanocrystals in KB44 (Nasopharyngeal carcinoma (NPC)(and treatment in head and neck malignance cancer and various biomedical applications [23, 32] can be inspiring for novel drug formulations.

This new presented study has identified a novel mixed of valuable NPs formulation as one of the newest techniques to synthesize a nanopackage fluid against various 6 cancers cell lines for the first time. This is a response to high needs for synthesizing of full-energetic smart surfaces in water-based formulations to suppress and destroy chronic and malignant cancer cells. It can be proved that association between several effective NPs and nanocomposites, and the design technology of smart hydrophilic surfaces of NPs are able to extremely inhibit the growth, proliferation, and survival of cancer cells. The key is that NPs/Nanocomposites produce a strong energetic synergistic anticancer activity during therapeutic methods for a long-time cancer treatment. Recently, we could indicate influence of novel engineered ZnO/CNTs@Fe3O4 nanocomposite's cytotoxicity in chronic myeloid leukemia CML-derived K562 cells for the first time, whereas the synergism effect of this triplet nanocomposites has been astonishing in the treatment of chronic leukemia [33]. Herein, the scope of this particular research is focused on the synthesis and application of a nanofluid containing multiple NPs like zinc oxide quantum dots, carbon nanotubes and aluminum nanocomposites as a powerful nanopackage for six commonly used anticancer candidates, showing minimal damage to the normal cells (HFF-2). Moreover, authors claim about the relationship between such anti-cancer nanoformulation with typical bacteria, virus (AIDS, COVID-19) and fungal biological systems. Because, very fine and small NPs crystallite size can diffuse and permeable to pathogenic cell membrane including some species of prokaryotes such as virus, bacteria, fungus, and cancerous cell lines, and subsequently produce oxidative stress through free radicals and reactive oxygen species (ROS) which is one of the probable mechanisms of this cytotoxic effect. Other pathways are ion-ion coulombic forces and electrostatic interaction and covalent bonds with amino acids into proteins in cell membrane at interface line [19,20]. They are able to make strong hydrogen bonding between hydrophilic surface of nanomaterials in nanofluid with proteins and cytoplasm and repairing DNA. Provided that, researchers can synthesize and formulate prominent surface-modified quantum dot NPs as one of the best essential basic of novel nanodrugs via the standard nano-chemical methods.

Experimental Section

Synthesis of Nanofluid Product as Anticancer Agent

A certain amount of ZnO NPs@modified-CNTs nanocomposite which was functionalizes with fatty acid (oleic or soya been acid) and synthesized by co-precipitation and hydrothermal method was then dissolved in 0.5-1.0 g hydrophilic ZnO quantum dot nanoparticles (Q-Dot NPs) [19,20]. Then they were mixed strongly, the polyethylene glycol as important pharmaceutical binder and coconut-ester as suitable dispersant and viscosity control reagent was added slowly in room temperature to the mixed solution. The obtained nanoformulation was dissolve in a mixture of distilled water in suitable polar solvents along with a nonionic surfactant as a (w/o) special emulsifier. These basic components were mixing under vigorous magnetic stirring, followed by ultrasonic bath condition due to achieving the stabilization of NPs for 4-8h in room temperature. Finally, 1.03 g silica doped Al2O3 NPs mixed oxides as a co-assistant and activator of surface of ZnO Q-Dot NPs was added to obtained formulation and pH nanosolution was adjusted at neutrality. In fact, we used of engineering nanosurface phenomena, obtaining strong surface energy in nanoparticles and being not decompose with gastric acid (stomach acid). Hydrochloric acid, potassium chloride, and sodium chloride in gastric acid play a key role in digestion of proteins and are capable to functionalize surface of all nanomaterials to produce hydrophilic property. Figure 1 demonstrates the systematic fabrication process of this nanopackage fluid product as a surprising nanomedicine technology, applied for cancer therapy.

Cell lines and Cell Culture

The A549 (human lung carcinoma), Huh-7 (hepatocellular carcinoma, human Liver Cancer Cells), A-375 (human melanoma cells, skin cancer), KB44 (human nasopharynx carcinoma cell line), MCF-7 (human breast cancer cell line), HT29 (human colon adenocarcinoma cell line) were purchased from the cell bank of Pasteur Institute of Iran. They applied in MTT assay in appearance of our fabricated nanopackage product in vitro in this work. These cell lines were grown in high glucose Dulbecco's modified Eagle's medium (Dmem, Thermo Fisher Scientific) with 5-10% fetal bovine serum (FBS, phosphate buffered saline, without Ca+2 / Mg+2, Thermo Fisher Scientific) at 37°C temperature, in the presence of 5% CO2 atmosphere, and 90% humidified air under a CO2 incubator (Binder, Germany). The supplemented medium refilled every other day and cells were sub-cultured to reach optimal confluency [19,20,34]. All the prepared

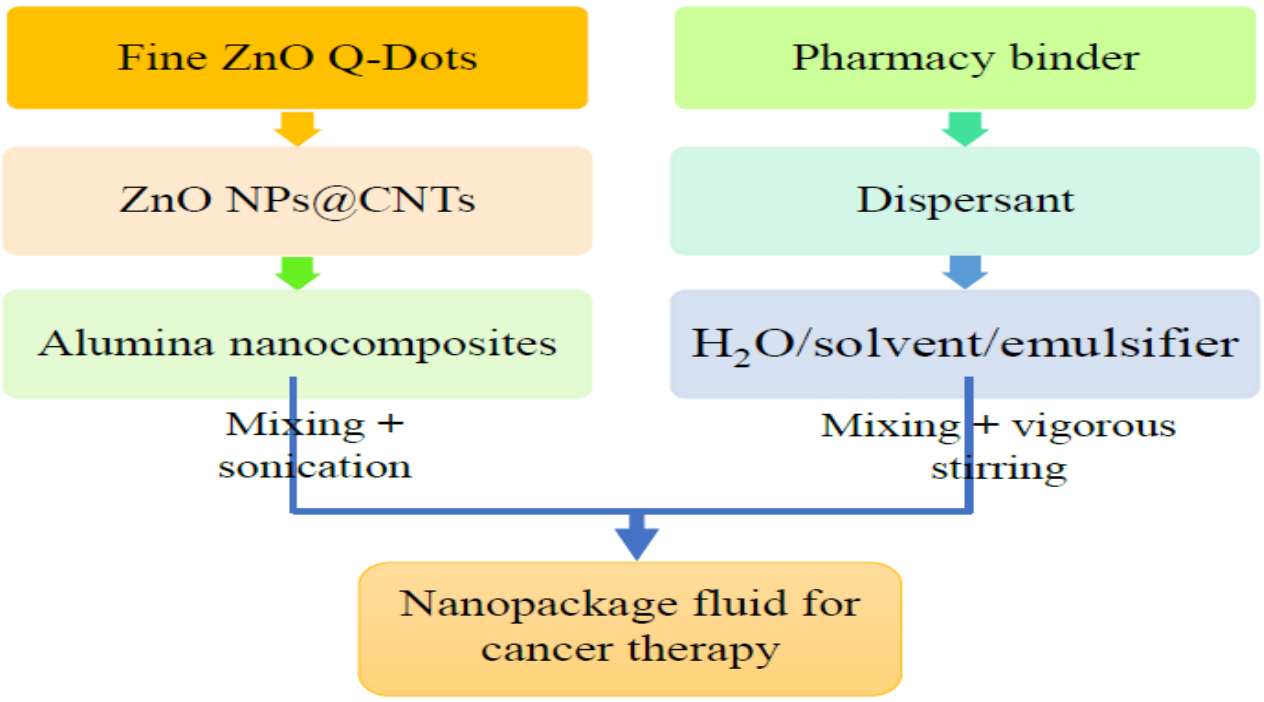

Fig. 1. A sample protocol diagram of production paths for our nanopackage fluid applied in cancer therapy.

Anti-proliferation assay (IC50 values)

The rate of cell viability or percent of cytotoxicity was assessed by the MTT assay, using various nanopackage fluid product concentrations (5, 10, 50, 100, 200, 500 µg/mL) according the current references [20]. IC50% were reported after 24 and 48 h and compared with HFF-2 normal cell. Briefly, 1×104 cells were seeded in 96-well Elisa plate in 90-100 µl supplemented DMEM the day before adding compounds. The day after, new nanofluid product concentrations were added to each cell population following the refreshing of the culture medium. Here, 48 hours after treatment, 20 µl of 3-(4,5-dimethylthiazol-2-yl)-2,5-diphenyltetrazolium bromide (MTT agent, Sigma Aldrich) reagent was dissolved in PBS to reach a final concentration of 5.0 mg/ml. Then, the obtained solution was diluted ten times with PBS agent, and was added to each well (100 of solution). This solution was then transferred to an incubator for 4 hours and subsequently replaced with formazan crystals ([E,Z]-5-[4,5-dimethylthiazol-2-yl]-1,3-diphenyl-formazan). Then 200 µl dimethyl sulphoxide (DMSO) sample was added to each chamber and mixed together gently. Finally, the prepared solution was kept at RT for 20 min to solve the formazan crystals within metabolically viable cells. The UV–Vis absorption spectroscopy was measured at 550 nm using an ELISA microplate reader (Bio Tek, USA). This is because, the formazan structure is spectrophotometrically analyzed at 550 nm. The percentage of viable cells was determined using the formula: % Cell viability = absorbance of treated cells /absorbance of untreated cells × 100. In order to determine the dose of nanofluid product that could result in proliferation inhibition in 50% of cells (IC50) the software GraphPad Prism 6 (GraphPad Software, Inc, CA, USA) was used for each of the cell lines, separately. The percentage of cell-growth inhibition was determined by comparison with the untreated control cells [19,34].

$$\%\ Cell\ viability = \left(\frac{absorbance\ of\ treated\ cells}{absorbance\ of\ untreated\ cells}\right) \times 100$$

Statistical analysis

All experiments and results of quantitative studies were conducted in triplicate and data were indicated as mean ± SD (standard deviation). Two-tailed t-test and variance (ANOVA) were used to determine the differences between viability of the various cell lines treated with nanofluid product using GraphPad Prism version 5 software (GraphPad-Prism Software Inc., San Diego, CA). The achieved results with p values < 0.05 were considered statistically significant in order to calculate IC50 value concentration response curve drafts, using the mentioned prism software.

Results and Discussion

Colorimetric MTT (Tetrazolium) Assay and Efficient Cancer Treatment

Cytotoxic effects and IC50 values of nanofluid formulation on A549 human lung carcinoma (lung cancer cell), Huh-7 hepatocellular carcinoma (human Liver cancer cells), A-375 human melanoma cells (skin cancer), KB44 (human nasopharynx carcinoma cell line), MCF-7(human breast cancer cell line), HT29 (human colon adenocarcinoma cell line, and finally, HFF-2 human foreskin fibroblast as standard cell lines in vitro were screened after 24 and 48 hours of exposure, which are shown in Table 1. According with obtained results, IC50 values (the effective dose that inhibits 50% growth) of Huh-7 (75 µg/ml), A549 (60 µg/ml), A-375 (90 µg/ml), HT29 (75 µg/ml), KB44 (65 µg/ml) and MCF-7 cells (50 µg/ml) were determined, respectively. HFF-2 human foreskin

fibroblast as reference also indicated 115 µg/ml after 48 h treatment. The strange effect of this nanoformulation in Table 1 showed that the essential basic of nanomaterials in this nanofluid could suppress the human cell lines of breast cancer (50 µg/ml), lung carcinoma (60 µg/ml), nasopharynx carcinoma (65 µg/ml), hepatocellular carcinoma and human colon cancer cells (75 µg/ml), and human melanoma cells (skin cancer) (90 µg/ml), respectively ($P<0.05$). In addition, the nanopackage was able to attack towards six mentioned cancer cell lines successfully and break down all the biological interactions and bonding at the cell membrane interface. The consequences of MTT assay (standard test) illustrated fantastic cytotoxicity in a dose dependent manner in all human cancer cell lines specially for MCF-7 (human breast cancer cell lines (50 µg/ml), human lung carcinoma (60 µg/ml) and human nasopharynx carcinoma (65 µg/ml), respectively, compared with the untreated control cell lines in vitro. So, a rapid enhance in nanopackage fluids towards development of nanomedicine drugs can give massive promise to develop therapeutic approaches against these six cancers and modern medicine. To determine the cytotoxicity effects of nanopackage (nanofluid) product on all six cell lines, MTT assay was carried out as shown in Figures 2-4. In fact, this is a very valuable advantage for a cancer nanodrug that can respond to all these dangerous common diseases. Besides, it is also economically viable, low toxicity, cancer targeting and also low dose during the treatment of patients in hospital. Therefore, the arrangement of this scenario including nanoparticles and nanocomposites in aqueous base to eliminate these six cancers was very logical, reasonable and a high-grade scientific research.

Cell Lines	Exposure time (hours)	IC_{50} (µg/ml)
Huh-7	24	115
	48	75
A549	24	95
	48	60
A-375	24	120
	48	90
HT29	24	95
	48	75
KB44	24	95
	48	65
MCF-7	24	85
	48	50
HFF-2	24	300
	48	195

Table 1. IC50 values obtained using MTT assay of nanopackage product on Huh-7, A549, A-375, HT29, KB44, MCF-7, and HFF-2 cell lines after 24 and 48 (yellow colors) hours of exposure.

According to Table 1, the effect of synthetic nanofluids on cell lines MCF-7, A549, and KB44 has been reported more than others, respectively.

Efficient cancer treatment and anti-proliferative effect of nanopackage on cell viability

Cytotoxic effects of nanopackage fluid product on Huh-7, A549, A-375, HT29, KB44, MCF-7, and HFF-2 cell lines after 24 and 48 hours of exposure, was derived from MTT assay including different concentrations (10, 50, 100, 200, 500 µM) and was carried out in Figures 2, 3, and 4(A), (B), respectively. In these diagrams, half maximal lethal concentration IC50 values were arisen from Table 1, and the results showed as the concentration increases, the cell viability (%) significantly decreases.

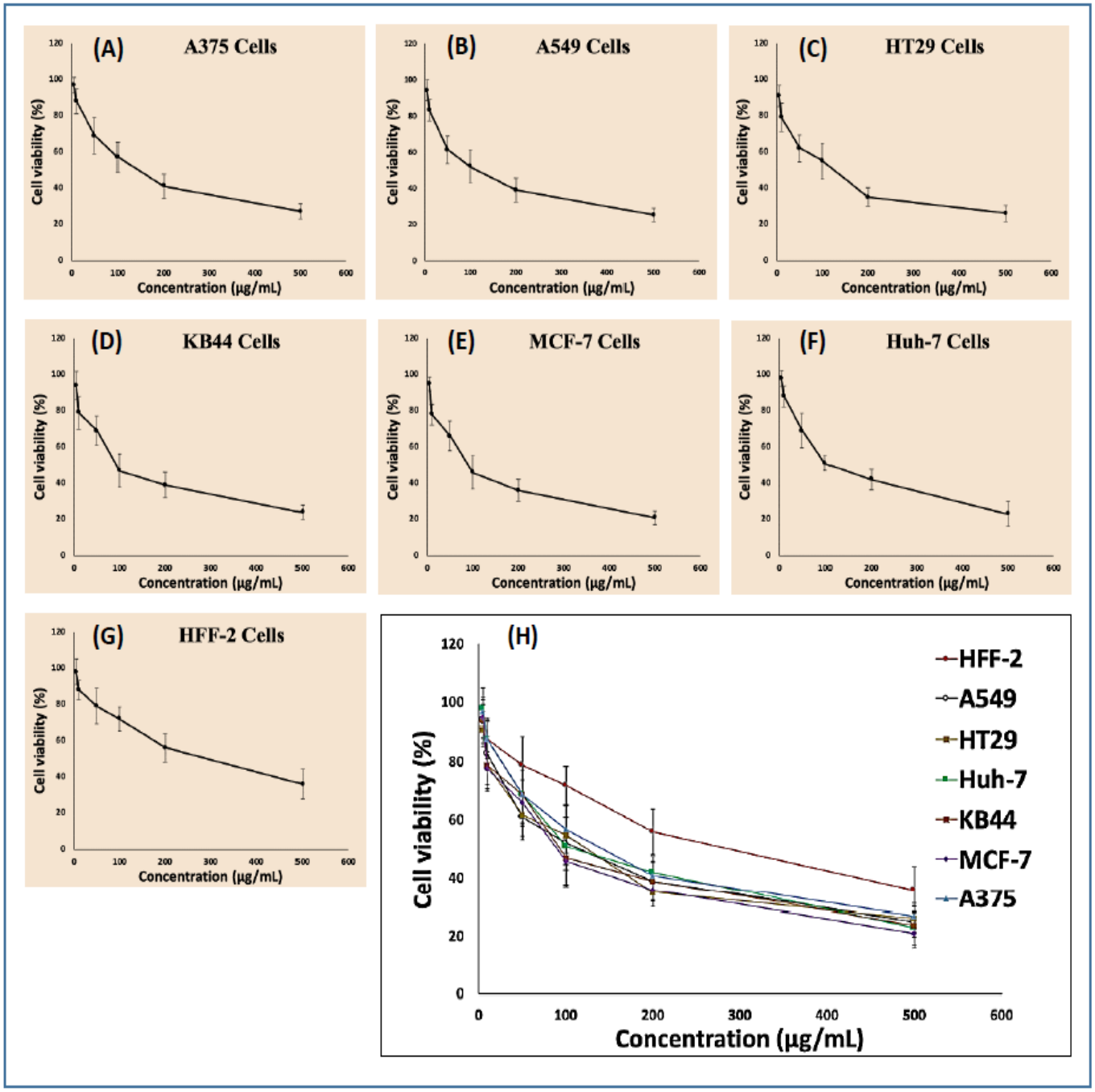

Fig. 2. Cytotoxicity effects (MTT assay) of nanopackage on (A) A375, (B) A549, (C) HT29, (D) KB44, (E) MCF-7, (F) Huh-7 and (G) normal human foreskin fibroblast (HFF-2) cells treated with various concentrations during 24 hours. (H) the MTT results of all the examined cell lines. The graphs showed that nanopackage has higher cytotoxic effect on the MCF-7 cell lines with IC50 of 85 µg/ml, while the normal HFF-2 diploid cells showed the lowest cytotoxic effect with IC50 of 300 µg/ml among all the analyzed cell lines. The values represent the mean ± SD and the experiments were performed in triplicate.

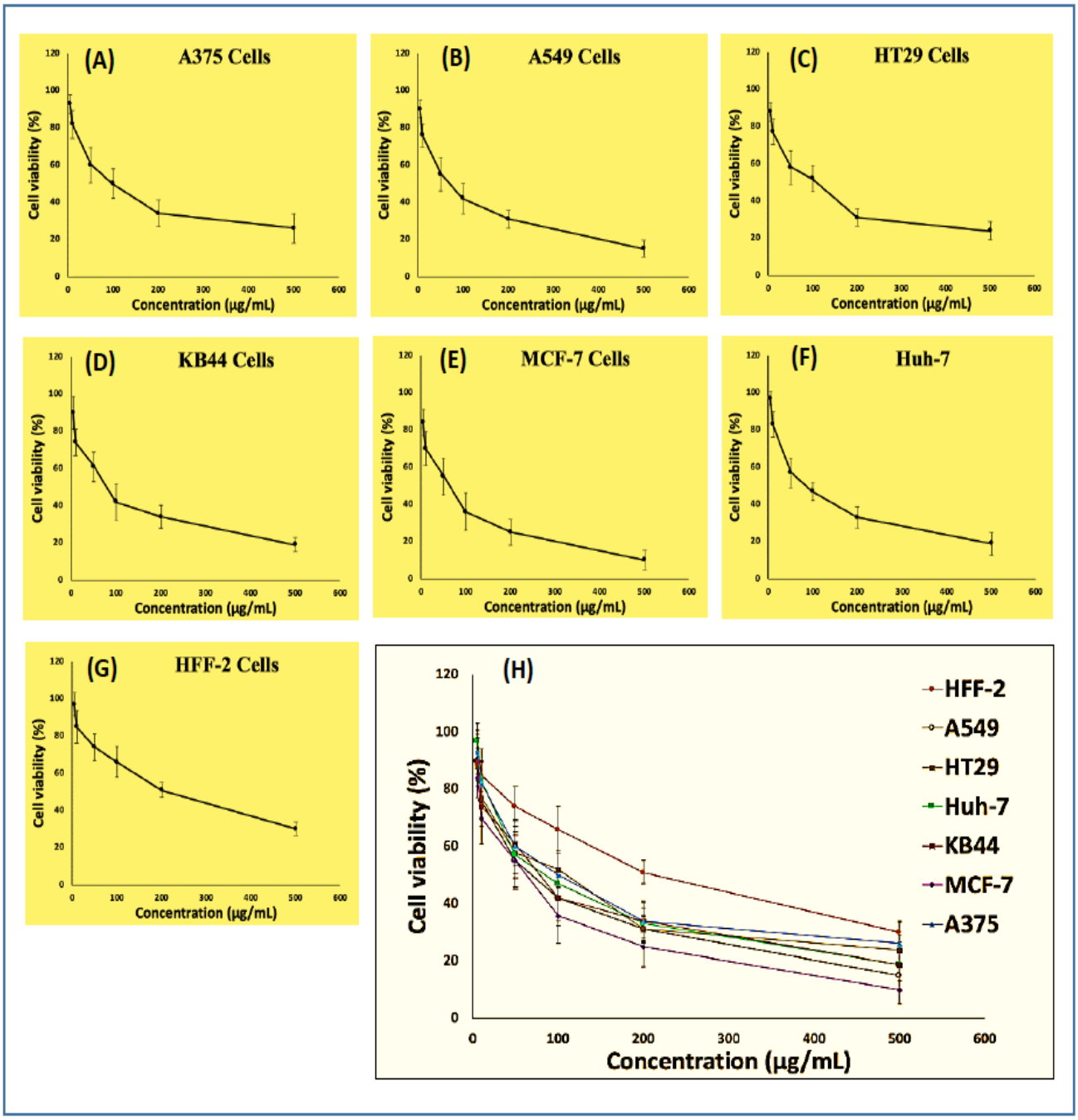

Fig. 3. Cytotoxicity effects (MTT assay) of nanopackage on (A) A375, (B) A549, (C) HT29, (D) KB44, (E) MCF-7, (F) Huh-7 and (G) normal human foreskin fibroblast (HFF-2) cells treated with various concentrations during 48 hours. (H) the MTT results of all the examined cell lines. The graphs showed that nanopackage has higher cytotoxic effect on the MCF-7 cell lines with IC50 of 50 µg/ml, while the normal HFF-2 diploid cells showed the lowest cytotoxic effect with IC50 of 195 µg/ml among all the studied cell lines. The values represent the mean ± SD and the experiments were performed in triplicate.

Figures 4 (A),(B), indicates all cell lines using various nanopackage fluid product concentrations (5, 10, 50, 100, 200, 500 µg/mL) in one diagram after 24h (A) and 48 h (B) of exposure.

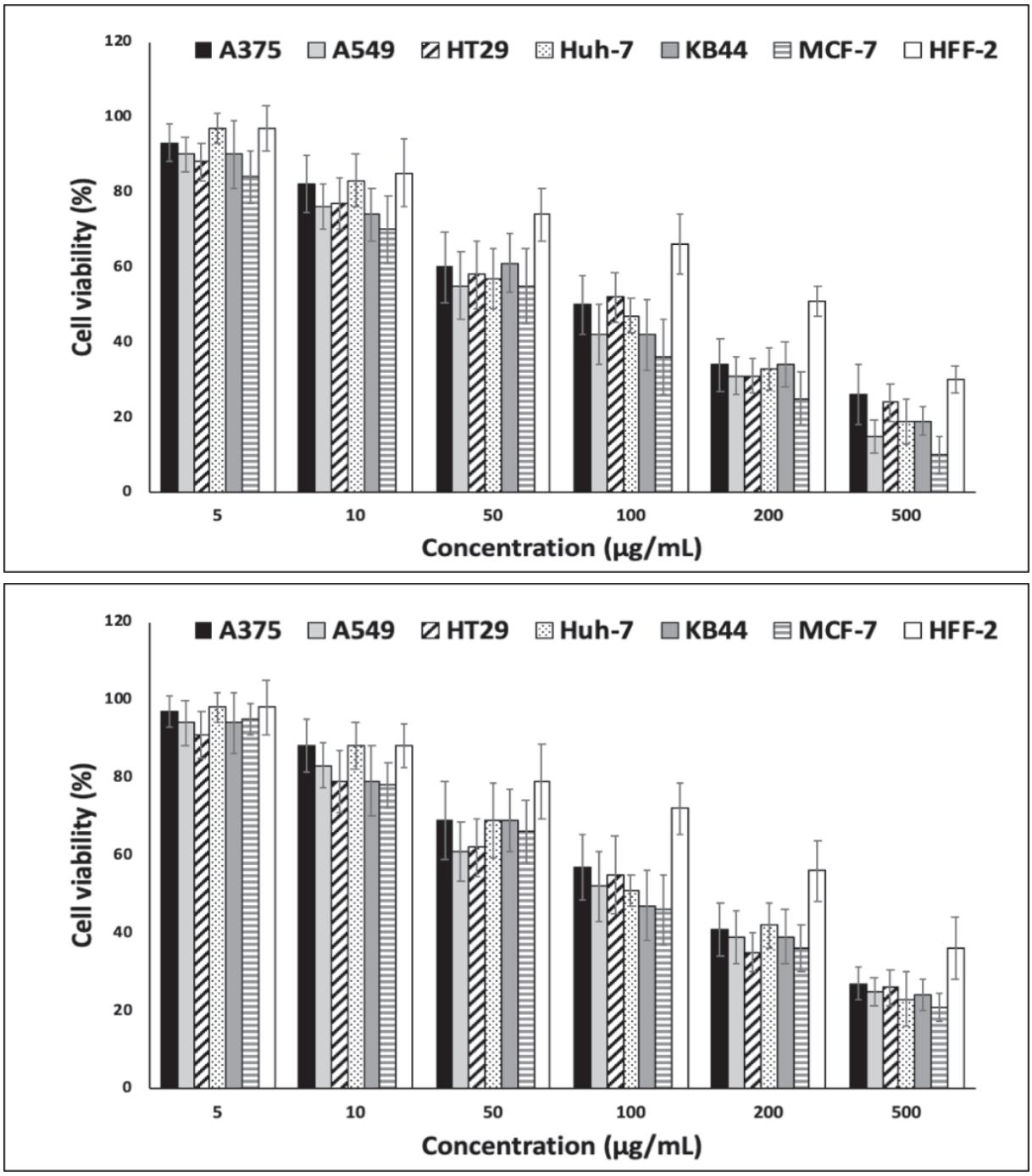

Fig. 4. (A) Cytotoxicity effects of nanopackage on the cell proliferation of all six different cell lines after 24 h and (B) 48h post exposure as column curves in comparison with control cells.

As shown in the graphs in Figure 2-4, nanofluid product growth inhibition works in significantly lower concentrations in all six cancer cell lines compared to normal cells. In accordance with the horizontal and vertical axes, all curves of six cell lines are rising and ascending under particular concentration conditions. With these results, it is therefore hoped that the performance and mechanism of the nanocomposites used in destroying the main function of applied cancer cell lines will be promising. Certainly, very well-selected nanomaterials could potently prevent the growth and proliferation of cancer cells without affecting normal cells.

Nanoparticles and nanocomposites in a nanopackage must have the ability to remain and stabilize in the bloodstream during the considerable treating time without being eliminated or decomposed, as they are targeted cancer cells. Furthermore, surface characteristics (surface modification with hydrophilic and hydrophobic domains), size of NPs, enhanced permeability of blood vessels in tumor cells, different configurations and retention effect, synthetic NPs should be an antineoplastic system and selectively kill cancer cells. For example, ZnO Q-Dot NPs are mostly environmentally friendly and have low toxicity and are considered to be safe in vivo and in vitro [35]. ZnO NPs@CNTs/fatty acid nanocomposites (metal–organic frameworks) and silica doped alumina NPs mixed oxides have important oxidizers agents and selectively target cancer cells and protect drugs from degradation and destabilization. They can store many cations such as Fe^{3+}, Fe^{2+}, Zn^{2+} and Cu^{2+} which are able to produce ROS (reactive oxygen species) via Fenton chemistry in lysosomes [36], hydrogen peroxide (H_2O_2) and hydroxyl free-radical production that act as the main attacking sites for cell degradation and subsequent cancer cell death. On the other hand, these types of engineered NPs antitumor were able to damage DNA (in mitochondria) in the MCF-7 line of breast cancer cells with the best IC50 in this study. It is possible that this event occurs directly or when they enter the cell membrane, they induce a cascade 3, leading to DNA damage (apoptotic processes). Authors suggest that this nanopackage product should be investigated further as in vivo animal experimental models. Basically, surface modified nanoparticles and quantum dot NPs induce oxidative stress in cells and damage them through the cell wall membrane permeability and DNA damage, producing destroyed textures and deformation cells, which eventually result in cell death (apoptosis) [37].

Characterization techniques of ZnO QD NPs in nanopackage product

SEM images of typical energetic surface modification of ZnO Q-Dot NPs

Field emission scanning electron microscopy (FE-SEM) (Zeiss, Sigma VP model, Germany) images of fine interesting shaped of nanopackage fluid are shown in Figure 5. Nanoparticles of fine ZnO Q-Dots (+50 mV, zeta potential) and others are found among the layers of instructive components and additives in the water-based nanofluid product. Multiwall CNTs (8-15 nm) which its surface was modified with fatty acid in the form of white beads are regularly seen in this nice picture. But at a larger magnification, these CNTs appear as thin white veins in leaf-shaped plates (left side image). Probably, spherical ZnO NPs have located over the homogenized CNT NPs in all the surface morphology. In better words, ZnO NPs are loaded on a suitable surface of CNTs and carried by them. Certainly, fine ZnO quantum dot NPs are scattered homogeneously everywhere and alumina nanocomposites are uniformly distributed between them.

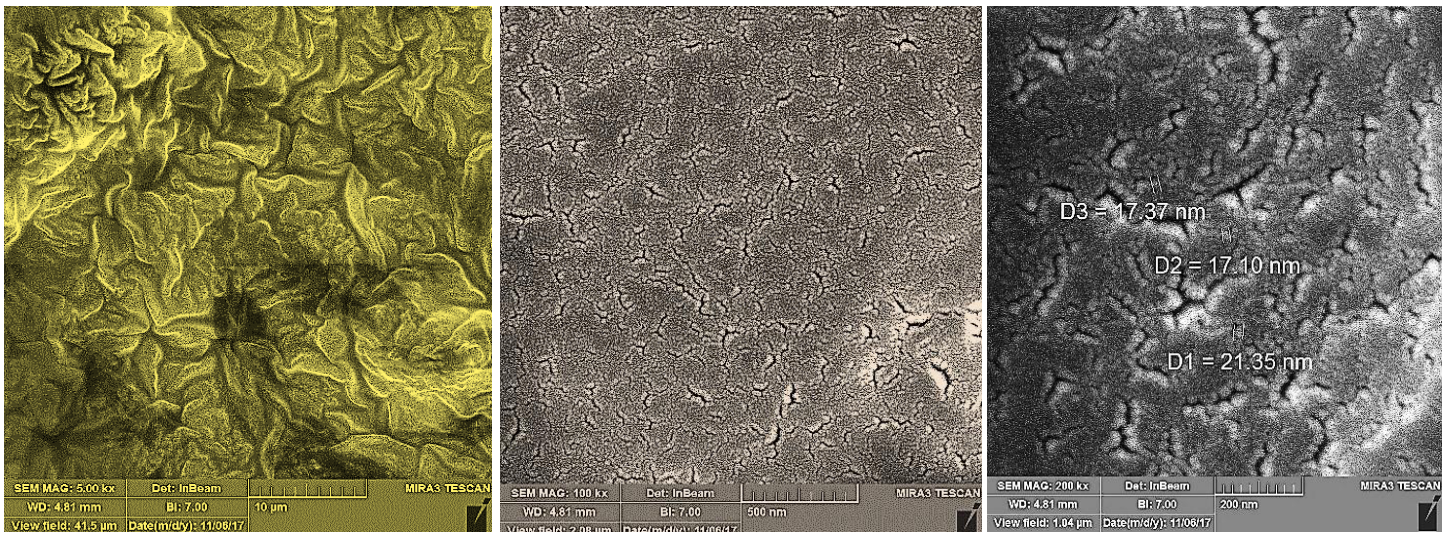

Fig. 5. FE-SEM images of spherical shape ZnO Q-Dot NPs in eco-friendly green fatty carboxylic acid layers, attractive CNTs nanocomposites and others in nanopackage fluid product.

It should be noted that, first of all, ZnO NPs @ modified-CNTs nanocomposites was achieved by co-precipitation, hydrothermal method, then its surface was functionalized with green fatty acid. Because its surface would be hydrophilic and soluble in water and with this idea, the nanocomposite will not be toxic and it is a very active and valuable candidate in nanomedicine.

EDS analysis curve for original nanopackage fluid product

Energy-dispersive X-ray spectroscopy (EDS or EDX) of dried nanofluid product was seen in Figure 6. The basic metallic elements in this nanofluid is clearly visible. According to this diagram, Zn (in ZnO Q-Dot NPs), Al (in alumina NPs) and Si (silica NPs as substrate) were shown similar to the synthesis of nanopackage fluid product. The wt.% for these basic elements are: C (43.43%), O (25.12%), Al (15.98%), Si (13.31%) and Zn (2.16%), respectively. The intensity and height of the peaks indicates weight % of these elements in dried nanoproduct. From this analysis curve we can be assured that the method of synthesis of NPs have correctly selected and the pure product has synthesized with no impurities.

XRD pattern of nanopackage product

The XRD (X-ray diffraction) pattern for the crystalized pure nanopackage product as dried powder with Cu-Kα radiation (λ= 0.15406 nm) displayed mixture of Wurtzite structure with hexagonal phase for ZnO NPs, and SiO_2 at 2Θ=20.688 according to reference pattern card number JCPDS No. 00-043-0596 crystal. These diffraction patterns could be indexed as typical structure as a-quartz phase. The type of crystal system was recorded hexagonal which contains space group: P3221 E and space group number: 154. Figure 7 shows XRD pattern of nanopackage powder as very wide and broad picks. According to the

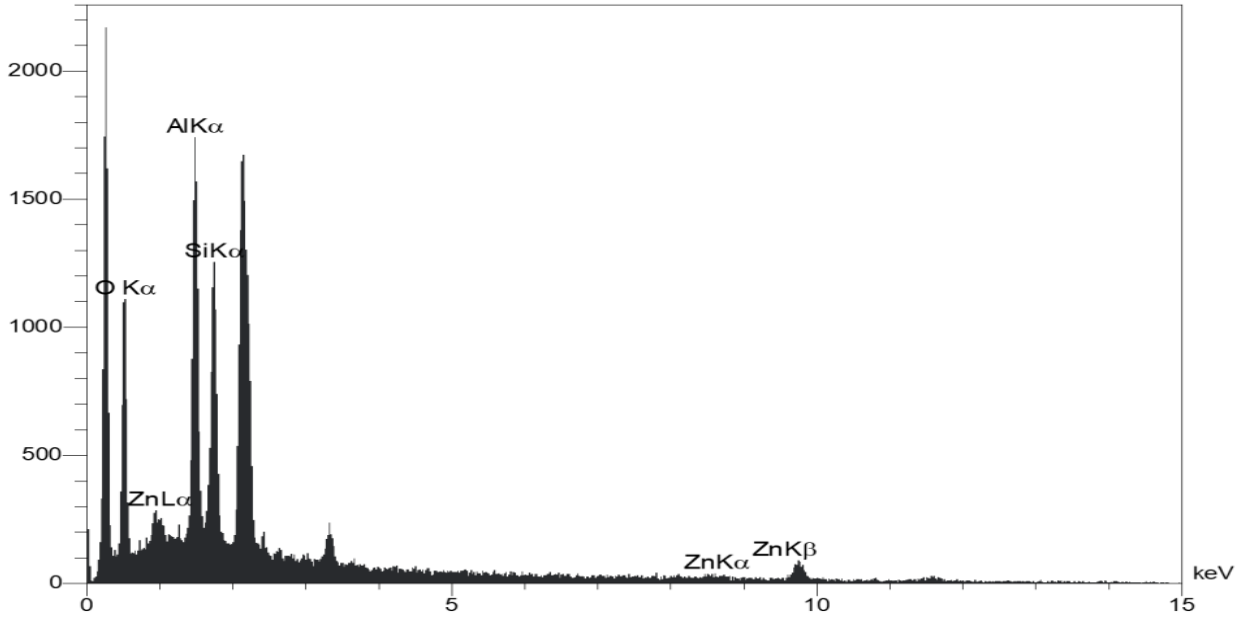

Fig. 6. EDX- profile curve for nanopackage fluid product in dried condition.

physics and quantum mechanics, when the peaks of XRD pattern are wide, the size of the NPs is small. Figure 7 presents very broadened peak in maximum curve for silica NPs (2θ =21). In addition, the NPs in nanopackage are generally small in size which it may has a mixture of fine-crystalline (amorphous) SiO_2 NPs (with random distribution and have no sharp peaks) and nanocrystalline (sharp Bragg peaks) phases. Certainly, the picks of various NPs may overlap on each other and is not related to fully amorphous nanomaterials. In fact, the Debye-Scherrer method and UV-Visible spectroscopy can be used for estimating the mean crystallite size. On the other hand, multi walled carbon nanotubes (CNTs) NPs (2θ =24) has characterized by many noises by XRD graph. Additionally, low peaks at scattering angles such as 32, 34, 36, 47 and 56 (2θ) correspond to the reflection (100), (002), (101), and (102) crystal planes respectively, for Wurtzite structure of ZnO NPs or ZnO Q-Dot NPs. However, the crystallite of powder nanopackage obtained from co-precipitation and hydrothermal method is ultrafine in dimensions [38,39]. Therewith, the different NPs in nanoproduct fluid are not perfectly crystalized and each part is oriented, differently. In the XRD pattern, there are not any sharp peaks as crystalline materials.

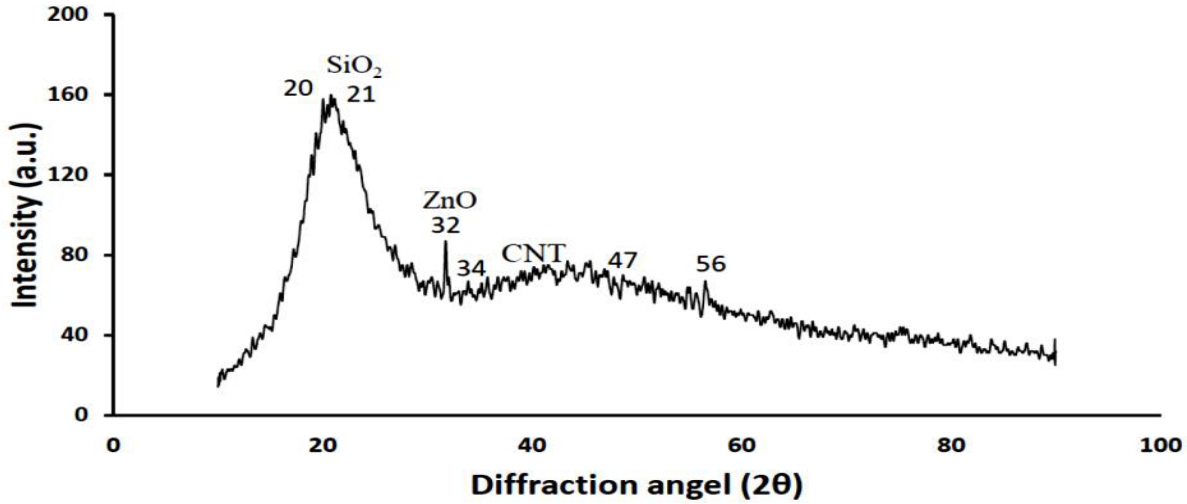

Fig. 7. XRD pattern of nanopackage fluid product in dried 80-100 °C.

FTIR spectroscopy of the original nanopackage fluid product

Fourier Transform Infrared (FTIR) spectroscopy (PerkinElmer, Spectrum Two model) in Figure 8 is fundamentally investigated in the range of 450–4000 cm-1 in the absorbance mode at room conditions. The original nanopackage fluid in KBr matrix showed a sharp pick with very high intensity at 3405.23 cm-1 corresponding to the vibration mode of water –OH group in H-bonded water and -COOH carbocyclic acid stretching bands belonging to fatty acid in nanoproduct. The very sharp band at 2860.00 and 2923.77 cm-1 associate to the –CH and –CH2 stretching vibration of alkane groups. The low pick at 1352.78 cm-1 related to carboxylic acid and zinc carboxylate (COO-) groups [20]. Two low intensity frequency bands at the range of 800.53 -886.72 cm-1 showed –OH twisting vibrations and lattice Zn–HO in defect structure of ZnO semiconductor NPs. The main stretching peak of interest in amorphous silica NPs observes as very sharp peak at 1111.06 cm-1 (Si–O and Si–OH) absorption bands and asymmetric vibration's peaks at 939.45 cm-1 and symmetric vibration of Si–O (795-800.53 cm-1) [40]. Usually, the strong absorption bands around 577 cm-1 can be described towards the stretching vibration of Al-O bond in the pure Al2O3 NPs sample which in this spectrum it has been assigned as a very low pick after 800.53 cm-1 [41]. The visible vibrational modes of multi walled CNT–COOH at 3405.23, 1735.50 and 1111.06 cm-1 are attributed to the O–H stretching, and C = O stretching carboxyl group indicates the presence of carboxylic group which was created during surface CNTs modification and finally C–O bending (which has overlapped with Si-O band), as well [42] (because of their proximity to each other).

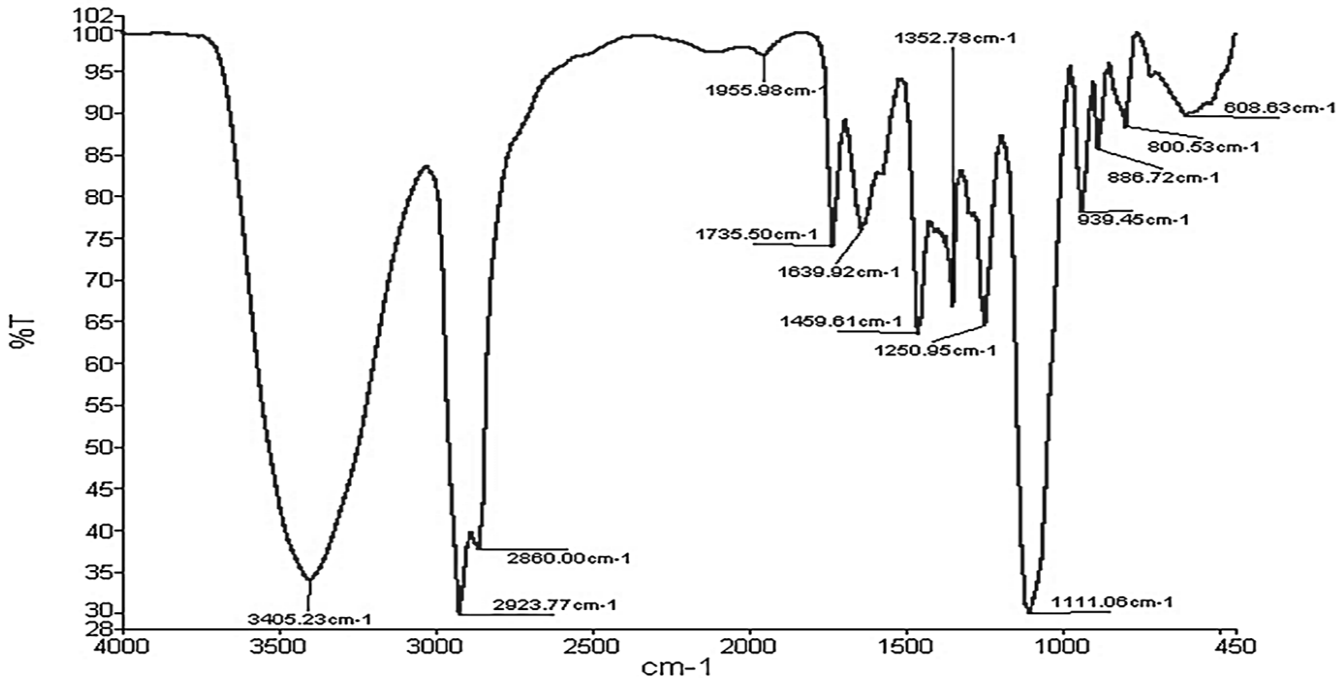

Fig. 8. FTIR spectroscopy of original nanopackage product with many absorption bands for mixture of ZnONPs@modified CNTs, ZnO Q-Dot NPs, and Al2O3 components in the nanofluid.

UV-Visible Spectroscopy of nanopackage product

In the present study, Figure 9 illustrates the UV-Visible (Perkin Elmer model lambda 35) absorption spectrum of nanopackage product as formulation of nanofluid. The absorption edge started in shoulder at around 199.04, 233 nm and followed by wavelengths at 245, 275 and 312 nm which are in ultraviolet-visible region (Figure 9(a), 9(b)). So, it can indicate blue emission due to oxygen vacancies and atomic reactive sites on surface modification of ZnO Q-Dot NPs, and CNT NPs due to the electron transitions from the valence band to the conduction band. These NPs have great wide special surface area, and many pours and have large band gap energy. So, mean particle size has estimated approximately to be small nanosized. The fourth max peak is observed at 312 nm in UV-Visible absorption spectrum (Figure 9(b)). Basically, there is the direct relationship between the optical absorption spectrum of fine NPs which cause by surface plasmon resonance and its broadening UV-Visible absorption in quantum mechanics and physic. On the other hand, it is simple way to predict indirectly particle size from UV-Vis spectroscopy. So, if the max absorption peak of NPs shifts to the lower wavelength, the particle size would reduce (blue shift) and vice versa. Furthermore, there is a direct relationship between the fine NPs and their broadness with low absorption wavelength in UV-Vis analysis. Moreover, since NPs size is so small, the electrons of the particles are in a very narrow potential (size of the NPs). According to the fundamental quantum statistical mechanics, whenever the width of potential energy barrier decreases, the energy level's distances increases. Because of that, the absorption peaks shifted towards higher energy (blue shifted). This theory is also known for XRD pattern for fine and small sized single NPs. From this information, it is found that although this nanoproduct is a mixture of several NPs in synthesis, but these are very fine nanosized particles. So, this interesting property is very valuable for a nanodrug in cancer treatment. Because, it can have strong diffusion towards the cell wall membrane without damaging healthy normal cells, working smartly. As we can observe UV-Vis in Figure 9 (a), it shows the short max absorptions at 200 to 389.0 nm and others are at 439.0 to 564.6 nm which are trapping states in curve. Therefore, it was found that, there are many different NPs with various absorptions wavelength in original nanopackage fluid product. This is a valuable advantage for nanoproduct and also confirms the synthesis method. Herein, a direct band gap (2.56 eV) was measured which was belonged to amorphous silica NPs.

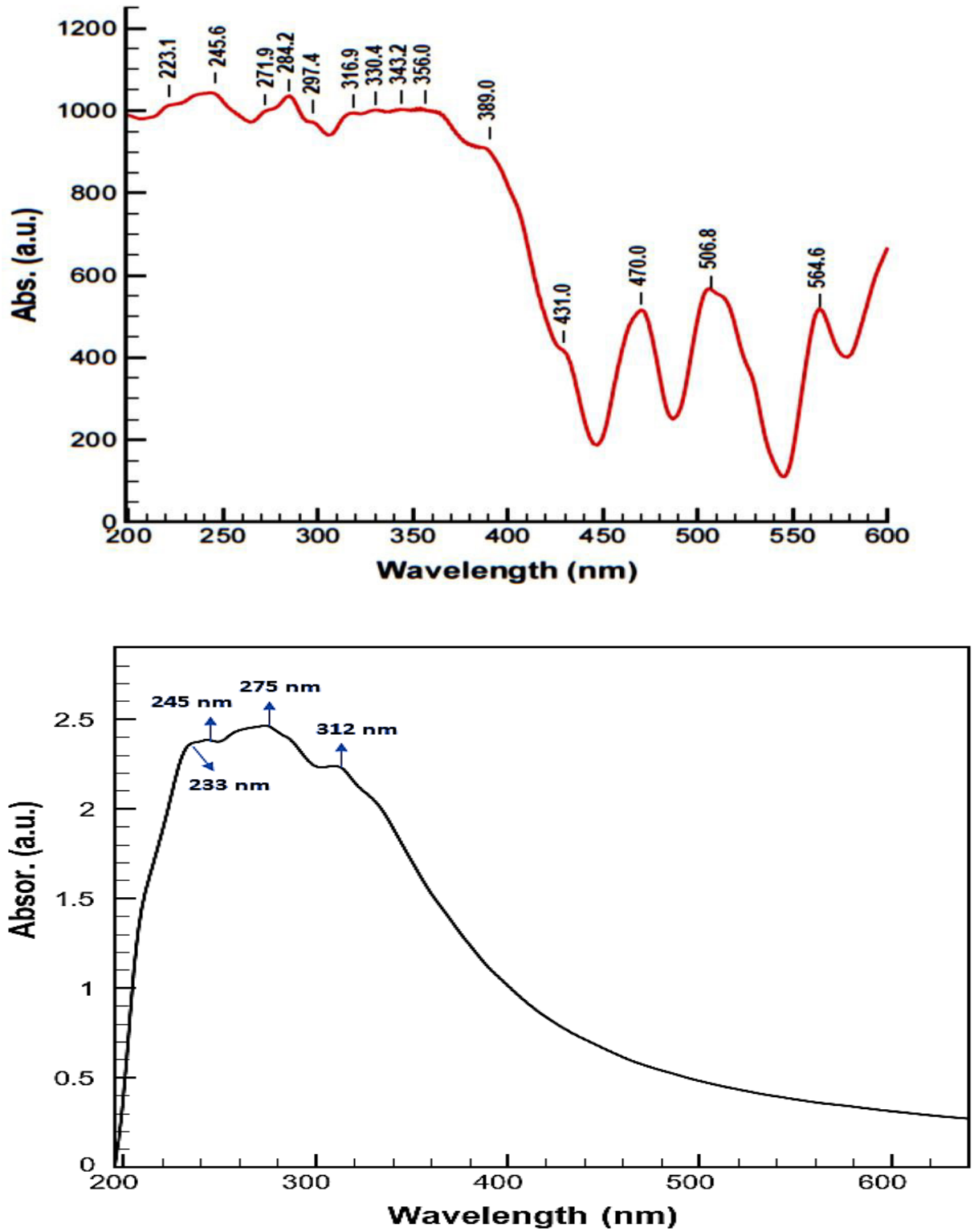

Fig. 9. UV-Visible absorption spectrum of nanopackage fluid product (a) at 200-600 nm contains a few low and high shoulders and broadening max picks which correspond to a blue shift, and (b) at 200-600 nm by removing trapping states it is possible to observe only initial max peaks in the spectrum.

Photoluminescence (PL) spectrum of nanopackage product at λ = 190 nm

Room-temperature photoluminescence (Varian model carry Eclipse) spectra of nanopackage product in water-based solution shows many trapping states and several splitting PL emission wavelengths between 448-580 nm under excitation wavelength of 190 nm. These quantized transition states could prove unique optical properties and blue emission at various wavelength 190 and 233 nm which herein we observe PL spectrum at λ = 190 nm (UV region) in Figure 10 PL spectrum corresponds to the near-band gap-edge excitonic emission of the ZnO NPs crystal. Moreover, single ZnO Q-Dot NPs presents photoluminescence emission in the UV-Vis region depending on the smart surface- modification, surface defects, nanosized regime, morphology, types of vacancies (ROS), shape, synthesis procedure, and electron-hole deep level. When semiconductors ZnO NPs combine with multiwall modified-CNTs -NPs, this hybridization process allows to improve more individually PL characteristics. This is caused by creating new trapping states as high ladder-shaped peaks, various defects, surface oxygen vacancies and engineering of the surface energy [20,43] for such nanohybrid material. Generally, the optical absorption spectrum of the very small NPs obtained using UV–Visible spectroscopy shows the blue-shift with decreasing particle size. Naturally, the value of band gap energy becomes large due to the quantization effect and small size of NPs [44]. Semiconductor NPs are able to generate various active free radicals, then, they are capable of absorbing the microenvironment around the involved cancer cells and produce strong electrostatic interactions with living tumor membrane cells at a biointerface. The morphology of these cell membranes at biointerface change and become collapsed and degraded.

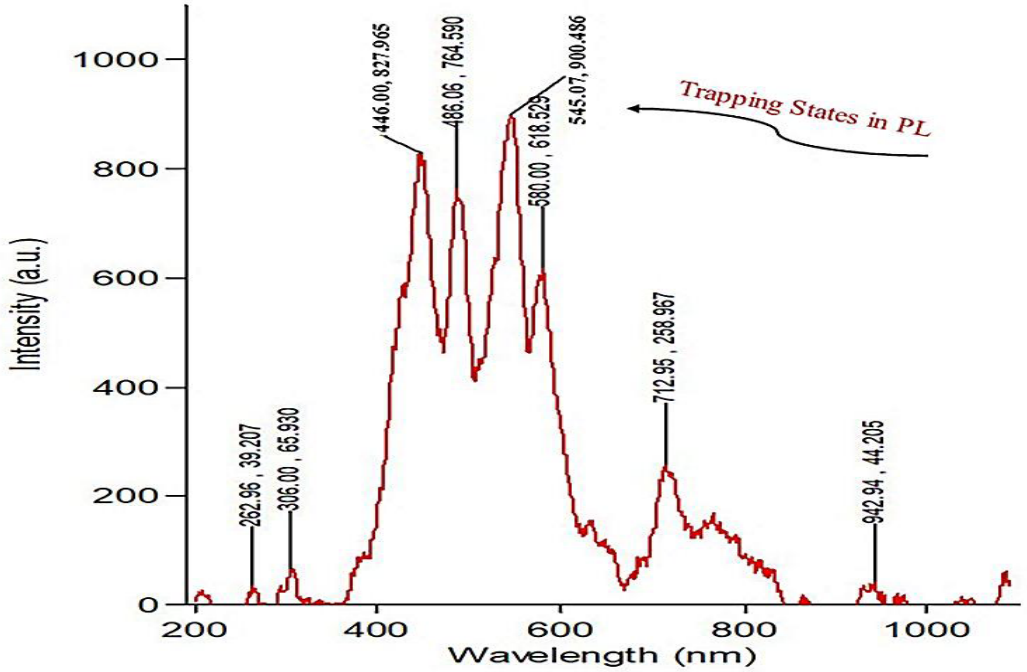

Fig. 10. Photoluminescence (PL) emission spectrum of nanopackage fluid product under excitation wavelength 190 nm. Trapping states as high intensity ladder-shaped peaks shift and broadening peaks are measured under UV radiation.

Biological application of nanopackage fluid product as a nanodrug in cancer treatment and investigation of mechanism and behavior of NPs and nanocomposites towards cancer cell lines constituents

Given the enormous problems that humans have today with a variety of microbes, bacteria and viruses, but advanced human knowledge can prevail over many of them. Since nanodrugs for the treatment or prevention of AIDS must be from oxidizing groups, therefore, it can be suggested that since the most cancer diseases are also arising from viruses, so synthetic cancer nanodrugs could be selected from the oxidizing groups, as well. Therewith, surface modification of NPs such as miracle ZnO Q-Dot fluorescent NPs and semiconductor single-walled or multiwalled carbon nanotubes (CNTs) NPs can be beneficial, because they can readily cross biological barriers, and can effectively transport molecules into the cytoplasm without producing a toxic effect [45]. Having a large surface area, stable nature, and unique optical and excellent chemical properties, ZnO nanopolymer (polymer-based NPs) and Al_2O_3/SiO_2 nanocomposites are really perfect options for this scenario. Because they possess particular properties such as, active pharmaceutical ingredients engineered within surface of NPs, individual structural characteristics, drug resistance, and specific targeting.

Relationship between virus and cancer cells and mechanism

Some of the activated chemical reactions that are destructive to microbes involves electron transfer reactions and the formation of various free radicals such as singlet oxygen (function of cytotoxic). Singlet oxygen can include the potent hydroxyl radical –OH^0 (a

powerful oxidizer) which is capable of directly destroying bacteria, viruses and fungi towards lethal peroxidative reactions. Anti-virus drugs (such as anti-HIV and anti- COVID-19) are most likely engage the redox chemistry group (based on our previous anti-virus studies (, just like the cancer nanopackage fluid product in this paper. Then, we claim that ZnO NPs have very great potentials in nanomedicine especially in the fields of anticancer, antibacterial, and anti-virus fields. Such NPs can generate reactive oxygen species (ROS) and free various radicals, release Zn+2 ions, and induce cell apoptosis in cancer cells. As a complementary supporter, surface modified-CNTs NPs used as redox agents. Depending on whether the surface of the CNTs NPs is modified with hydrophilic or hydrophobic agents, it can perform oxidative and reductive reactions (redox reaction). So CNTs NPs are great candidates for fighting against viruses or cancer cell lines. On the other hand, semiconductor alumina (Al^{3+}) NPs and their surface modification are strong oxidizers and can induce DNA fragmentation, being one of the significant markers of programmed cell death [46] ($Al^{+3} + 3e^- \dashrightarrow Al^0$). SiO_2 structure has a tetrahedral arrangement with one silicon bonded to four oxygen atoms. It can oxidize and also has a very porous structure. According to the chemistry science, oxidizing agents must be able to accept electrons readily such as the elements with high electronegativity or some metals which have high oxidation numbers (Zn^{+2} and Al^{+3}). Moreover, when an oxidizing agent removes electrons from a molecule, the chemical structure of the molecule is changed, and the physical properties (like color) are altered. Free radicals (from ROS process) are intermediate chemicals that have a short lifespan. They contain one or more unpaired electrons in their last layers. For this reason, they are very chemically reactive and for getting necessary electrons, they attack the adjacent stable molecules, and stimulate them to be oxidized. A molecule that has lost its electron, can transform itself into a new free radical and this cycle continues. The oxygen molecule is essential for survival but its metabolites like ROS and oxidative stress must be constantly inactivated, therefore, in this situation only a small amount of oxygen molecule which is required for normal cell function would remain. However, a free radical can also act as a reducing or oxidizing agent. The most common reactive oxygen species (ROS) that are raised in biological systems including: $O_2^{\bullet-}$ (superoxide anion radicals, being not highly reactive, and generated as a byproduct of energy metabolism from mitochondria), H_2O_2 (hydrogen peroxide), $ROO^{\bullet}$ (peroxyl radical), $HOO^{\bullet}$ (perhydroxyl radical), $OH^{\bullet}$ (hydroxyl reactive radicals) and organic radicals ($R^{\bullet}$). This information keeps and supports the hypothesis that mitochondria as the major endogenous source of O2– contributes to physiological aging, provoking oxidative damage and apoptosis [47]. Finally, ROS groups increase aging due to their capability to attack cellular constituents such as DNA, protein and lipids. Therefore, ROS can also oxidize proteins and lipids, and also induce several damages to DNA. In addition, ROS agents, reactive nitrogen species (RNS) such as nitric acid (NO), and also nitrite peroxy (PN) play an important role in the mechanism of oxidative stress. Thereby, a specific series of NPs, can produce ROS and cause serious and hereditary damage to DNA, unlocking the spiral DNA structure and exposes it to any changes. Also, the mitochondrial genome is significantly vulnerable to oxidative attack. Scientists have shown that high levels of ROS cause the breakage of outer and inner cell membranes of mitochondria. This results in the release of the cytochrome c (Cyt c) protein from the mitochondria and activation of the cascade of bio events and stimulation of apoptosis [48]. Thus, ROS acts as an important mediator in the process of apoptosis. Furthermore, mitochondria are one of the major sites of ROS production in the cell, and for this reason, DNA is subject to oxidative attack. This is because, DNA polymer or nucleotides molecules contain four types of the phosphate group, a sugar group and a nitrogen base with the particular orders which can be disturbed and broken by free radicals, H_2O_2 and oxidative stress and disarrange the hydrogen bonding in their double helix structure. Figure 11 shows the schematic representation proposed for the actual action mechanisms of starting nanomaterials in presence of valuable chemical reagents. Three basic materials such as ZnO NPs@ modified-CNTs, ZnO Q-Dot NPs in aqueous solution, which generate esterification reaction and Al_2O_3@SiO_2 can be found in this diagram. The R-COO-ZnO Q-Dot NPs was added to co-assistant (alumina@silica) nanocomposites in mixture of binder, dispersant, emulsifier in water solution. Interestingly, all of these nanomaterials could create strong synergism effects in a nanopackage.

Biologic Redox Reaction:

Among problems that cancer cells produce, there exists the breaking of the covalent S-S bond (disulfide bridge). Disulfide bridges are formed between thiol groups in two cysteine residues of proteins which have been broken to free sulfhydryl (S-H) radicals during the reduction reaction.

R-S-S-R + ne^- (number of electrons from virus, microbe, or cancer cell lines) $\longrightarrow$

R-SH + SH-R (reduction chemical reaction), (**thiols**)

S– anion from one sulfhydryl group acts as a nucleophile, and in the process, it releases electrons (reducing equivalents) for transfer. The reduced substance causes oxidation and is therefore called an oxidizing agent (R-S-S-R). If oxidation-reaction occurs RS-SR would re-create.

($2\ RSH \dashrightarrow RS\text{-}SR + 2\ H^+ + 2e^-$) (oxidation chemical reaction, by **nanoparticles**)

therefore, R-S-H is reducing agent in redox reactions [49].

Intramolecular and intermolecular reactions occur in disulfide bonds for stabilizing tertiary and quaternary protein membranes. Two cysteine residues can be connected by a disulfide bond (S-S) to form cystine and have a key role in protein folding and stability. Disulfide bonds such as nanoparticle oxides are used in many processes, including DNA replication. So, can act as an oxidizing agent, oxidizing the thiol group on a protein.

Experiences have shown that most bacteria and viruses break down valuable disulfide bonds, then strong NPs with high surface energy as the oxidizing agent can re-bind these open bonds. This is where the surface-modified NPs types and the production of free radicals and their oxidizing role are crucial (in oxidation-reduction reactions). Moreover, the virus (like corona virus) can be a living organism including a lipoprotein molecule which has covered by an outer lipid (fat) layer (lipoproteins are also present in cell membranes, mitochondrial, chloroplast membranes, and bacteria). The virus is not killed but can collapse alone and decay and finally break down in the appearance of free radicals, H_2O_2, heating media, and using the solubilizer or hydrolysis of the fatty layer (saponification reactions). In addition, in this mechanism and from the viewpoint of chemistry founding, virus donates extra pathogenic electrons to disulfide bonds in protein and reduction reaction occurs, thus, sulfhydryl (S-H) radicals would be generated. NPs can help to break virus' cover proteins, by inducing extra destructive electrons and producing RS-SR again which are crucial roles in various cellular processes. Herein, as a very interesting result in this event, great NPs, strong nanofluids and a new nanopackage have very influential roles in reconstruction and repair of disorganized covalent bonds of DNA-protein cross-links.

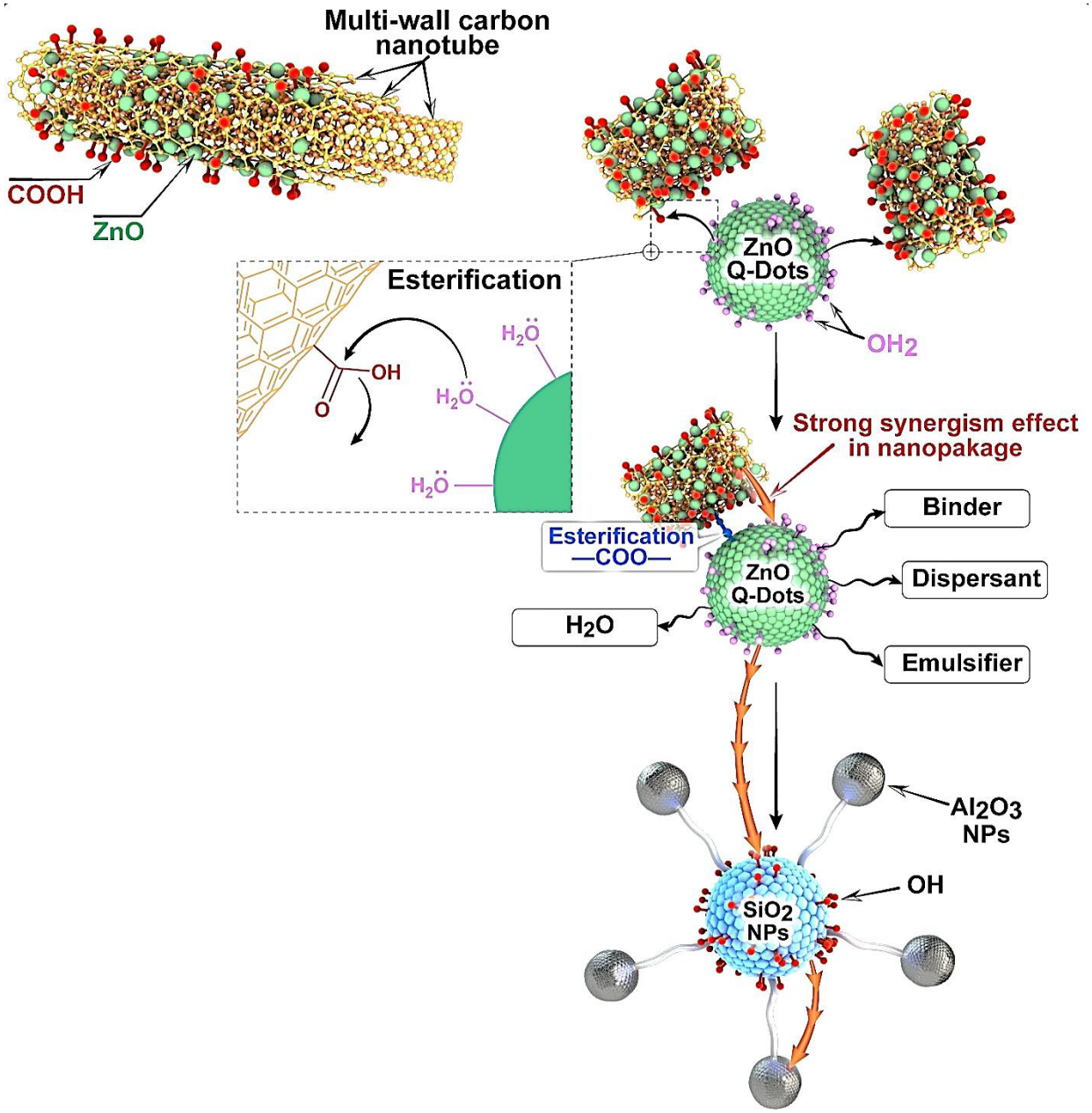

Fig. 11. The infograph of the basis nanocomponents and important reagent solutions in our nanopackage. Synergistic properties were observed between ZnO (over CNT), ZnO Q-Dots, SiO_2 and Al_2O_3 NPs. Esterification has been manufactured between –C=O (carboxylic) and O-H (H_2O) which causes full stability between ZnONPs@modified CNTs and ZnO Q-Dot NPs in a synthesized liquid solution.

On the other hand, NPs are able to wrinkle and deform texture of cancer cells which is a significant sign of apoptosis and eventually damaging [19]. It is also hugely important that they do not allow the mentioned destructive factors to destroy the healthy normal cells of the human body as intolerant side effects in conventional chemotherapy treatments. These evidence and major vital chemical reactions were observed in Figure 12. It can be seen in these biological pathways that cancer cell lines, bacteria and virus have ability to denature cystine residue's covalent linking to two thiols or mercaptan (R-SH) in cysteine (Cys) and glutathione in proteins. Thiols have illustrated specialized properties (high affinity metal binding, nucleophilicity, redox biology reaction, and ability to form disulfide bonds). It can be deduced that a full chemical reaction is derived from coordinated reduction (gain of electrons) of one species and the oxidation (loss of electrons) of another (electron transfer between dithiols and disulfides). Strong NPs can play as oxidative groups for reducing disulfide bonds, and suppress essential species of prokaryotes, since disulfide and hydrogen bonds provide important contributions in stabilizing the oligomeric protein-folding structures against unfolding and denaturing tragedy. This is a shift in the mechanical unfolding pathway.

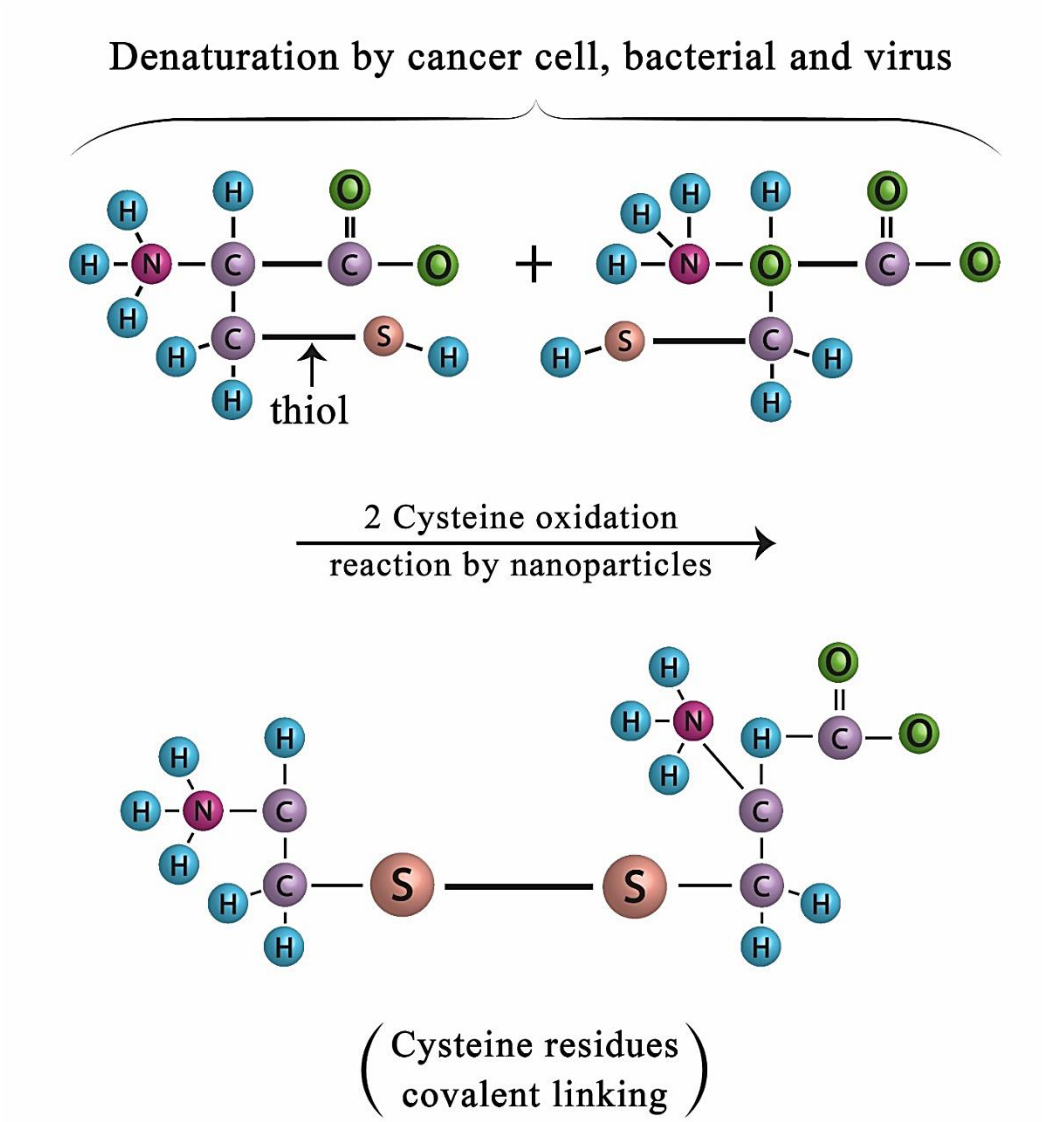

Fig. 12. Proposed mechanism of induced oxidative and reductive processes (thiol.... disulfide) by strong surface energy of smart NPs specially ZnO Q-Dots in biological systems and proteins stability. The important impact of disulfide bonds on protein misfolding/protein stability and human diseases underpins the base of our proposal.

Oxidation-Reduction Reaction for Nanoparticles

We should understand that what key functions should be oxidized and what factors should be reduced. From this perspective, very good oxidizing and reducing NPs and nanocomposites can accomplish this mission and task. Except such main parameters, it has been proven that, there are many other factors in a nanoformulation design, such as: size of NPs, permeability, concentration, pH of nanosolution, solubility, the stability of NPs in nanofluid, shape, geometric structure of NPs, surface charges (zeta potential), positively charged NPs, power of cell membrane adsorption, transport of particles in the nanofluid, electrostatic interaction between the cells and the NPs (cell membrane is negatively charged), nanoparticles-to-cell attraction, dispersion of NPs in the culture medium. Therewith, the connection type of NPs to the protein, adsorption between NPs and cell membrane [50], avoiding the decomposition of NPs in the blood (nanodrug resistance), efficacy, toxicity, smart targeting specificity, and finally good biocompatibility are significant key variables which are still observed in this category. There is one big opportunity herein: the power of surface functionalization of NPs to be specially designed according to our needs and wishes. Simultaneous tumor targeting by NPs and water-based nanofluid allow prolonged blood circulation time and control drug release in the human body. Most breast tumor cells are located at the plasma membrane or alternatively at the nuclear membrane [51]. Accordingly, with experiences of nanotechnology science the fine NPs in water-based nanofluid which modified by active biomolecules such as nucleic acids, sugars, peptides, lipids and antibodies can actively diffuse and bind to cancer and tumor cells through cell wall membrane at the interface between them. Then, NPs with great affinity selectively combine with molecules of proteins, folate, sugars, transferrin, and aptamers or lipids and finally release

into the cytoplasm which include folic acid, albumin, and cholesterol ligands. Because the high special surface area of very small NPs, cancer cell lines spread on the wide surface of NPs and adsorb over their nanoporous and trap in them. In this processing, the oxidation-reduction reaction causes that reactive oxygen conductivity to be disturbed and then the special bonds of viruses' structure would be broken (cellular dying via process called apoptosis) [23]. Besides, NPs have significant properties to minimize damages and decrease the cytotoxicity on non-cancer cells [34] which is one of the best advantages to use NPs for cancer treatment or potential destroying and killing the human virus infections (SARS, MERS, and COVID-19). Figure 13 shows all these biological pathways relevant with our nanopackage and tumor cancer cell at the interface. Strong hydrogen bonds between NPs and amino acids of proteins create wonderful phenomena in modern nanomedicine. In figure 13, three arrows (1, 2, 3) demonstrate the attack and diffusion order of NPs in case of their sizes and shapes. ZnO Q-Dots NPs attack the cellular membrane and diffuse into it, initially. ZnO Q-Dots can produce ROS and possess (e^-–h^+) with strong surface energy. Their particle sizes are very fine, as well (arrow 1). Secondly, Al_2O_3/SiO_2 nanocomposites attack, diffuse into cellular membrane and based on their enough concentration, they continue their diffusion and destruction of cancer cellules (arrow 2). When the concentration of these two agents would be finished, the nanocomposite no. 3 engages as supporter and continues the destruction process until the cancer cellules would be entirely destroy (arrow 3). The NPs are responsible for remediation and reconstruction of the damaged deoxidized S-S bonds in proteins via oxidation-reduction reactions. Each of the single NPs that are finer in size, can attack the cancer cells sooner, due to stronger surface energy. Such fine NPs have a more significant and more sensible role in the nanopackage against invasive cells. Thin film of tumor cell line at interface consisted of hydrophilic amino acids in its protein and lipid in cytoplasmic membrane in cancerous cell line of DNA. Smart NPs are able to move and diffuse very fast and reach to these membrane cellules and attack all species cell. They can recreate broken chemical bonds by redox reactions but not bombardment. Of note, the expression of atomic bombardment of aggressor cells is not true at all, because what is happening is just a chemical reaction.

In last part of Figure 13, strong and significant intermolecular hydrogen bridge bonds (H… O, NH… O, C=O… H, and N… H) is observed between the hydrophilic, very smart ZnO Q-Dot NPs in a liquid solution, having typical amino acids. This is a good sign to create a strong biological relationship between NPs in the role of rescuer with destructed species in the body such as destroyed proteins. Finally, energetic and effective NPs can reach to cytoplasmic membrane through diffusion and vital hydrogen bonding formation. Accordingly, the more stable crucial bonding, the resistant NPs will have high mobility due to having strong surface energy. Such potential mobility would display prodigious therapy. We also re-highlight that NPs were used at the lowest concentrations, which is highly important.

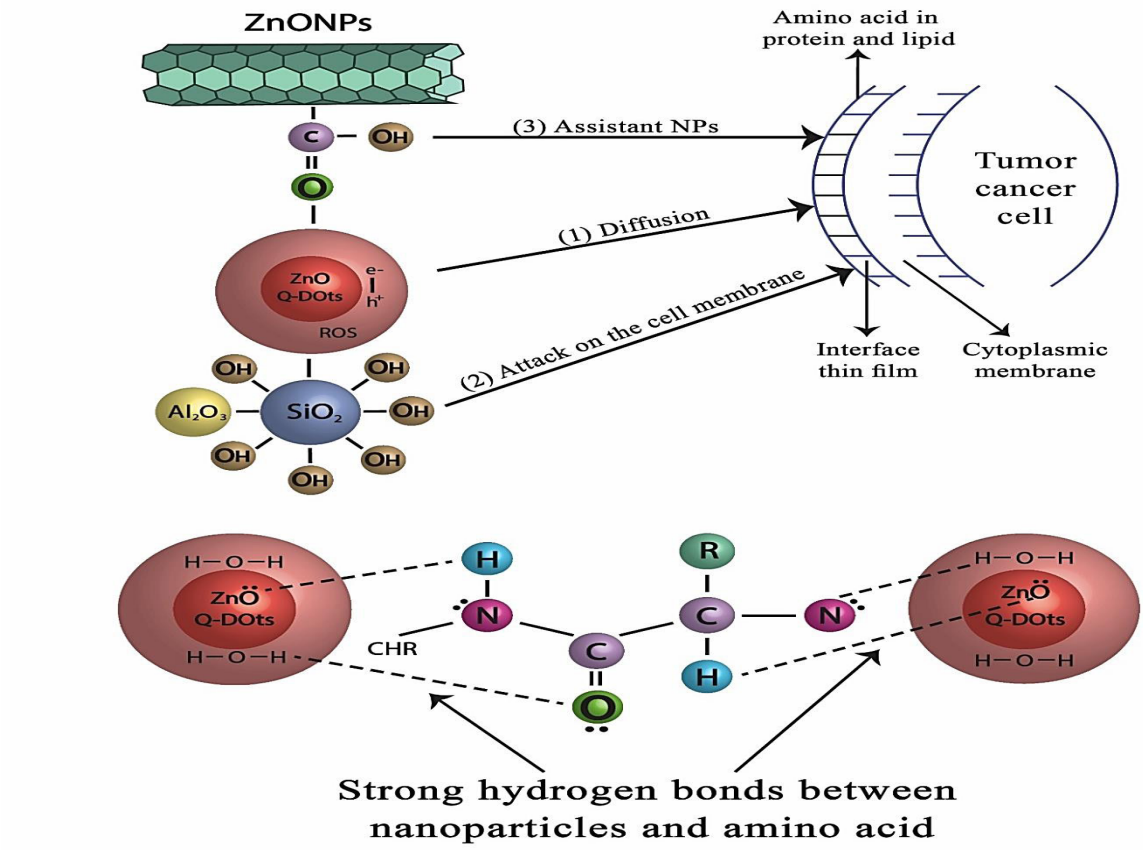

Fig. 13. Schematic representation proposed for attractive diffusion proceeding of three engineered surface modification of NPs into tumor cancer cell, and hydrogen bonding formation with membrane' amino acids in proteins and lipids (including fats, oils, and hormones).

Cancer cells, Virus and Bacteria

In recent years, authors had thought about the synthesis of novel NPs in water-based solutions for different anticancer drugs and their relationship as an antibacterial and antifungal [19,20]. It was shown that, ZnO NPs (particularly, ZnO Q-Dots NPs) with proper surface engineering, were able to selectively target and killed cancer cells, bacteria, viruses (AIDS), and fungi in desirable concentration, making them promising powerful agents in nanomedicine and biomedical industry. When very small NPs can diffuse inside the cell nucleus and bind to the components of cytoplasm, lipid vesicles, mitochondria, nuclear membrane, and DNA, they would be able to destroy all extravagant and unreal branches that have been made by virus or bacteria in the cytoplasm. Here, authors suggest an idea that, due to the biocompatibility of ZnO NPs and fantastic nanofluid derivatives, and similarity in process of destruction of biological systems in the body, modern and strong anti-cancer nanoformulations can also be used for other microorganisms (bacteria, virus, and fungal) [52]. We previously investigated using modified zinc oxide quantum dot NPs for breast and colon cancer cell lines and also various bacteria and fungi in 2014 [19]. In this regard, several bacteria such as *Bacillus anthracis, Staphylococcus aureus, Klebsiella pneumonia*, and *Staphylococcus* epidermidis bacteria were considered by this effective NPs in vitro. Also, different current opportunistic fungi such as *Microsporum gypseum, Microsporum canis, Trichophyton mentagrophytes, Candida albicans,* and *Candida tropicalis*, were evaluated and compared with the standard antibiotic agents like *Gentamicin* and *Clotrimazol* in this work. As a successful research, ZnO quantum dot NPs indicated potentially many unique and extraordinary properties as an antifungal, antibacterial and anticancer reagent. In another paper, we worked on ZnO Q-Dot NPs as a new nanomedicine proposal for evaluation of four cancer cell lines in vitro and continued over the considering its side effects using the animal model in vivo [20]. Overall, it can be concluded with reasonable confidence that the potent anti-cancer nanomedicine is able to respond definitely to other biological systems like viruses, bacteria and fungi (biological systems show intense synergistic effects). Figure 14, reveals the disulfide (S-S) structure in protein and lipid of living organism which are kept oxidizing by various biologic cell species in nature. These harmful cell biology species (reducing agents) are caused that S-S bonds break and change to R-S-H (thiol) [53]. Tumor cell, virus, bacterial, and fungal are special biological agents which attack and also damage immune system and human life. In this work, authors do research on different six common cancer cell lines. These cancerous cells can diffuse in cytoplasm and vital protein in human body and destroy fundamental bonds in its DNA. The engineered surface of NPs in a new synthesized nanopackage could with cancer cells with high potency. Noteworthy, thiols lose their electrons and become oxidize, but vital S-S covalent bonds are made again by strong NPs. Therefore, it is necessary for today's pharmacists and scientists to realize the importance and the miracle of NPs, and to make good use of this great industry in the manufacture of their medicines and clinical usage.

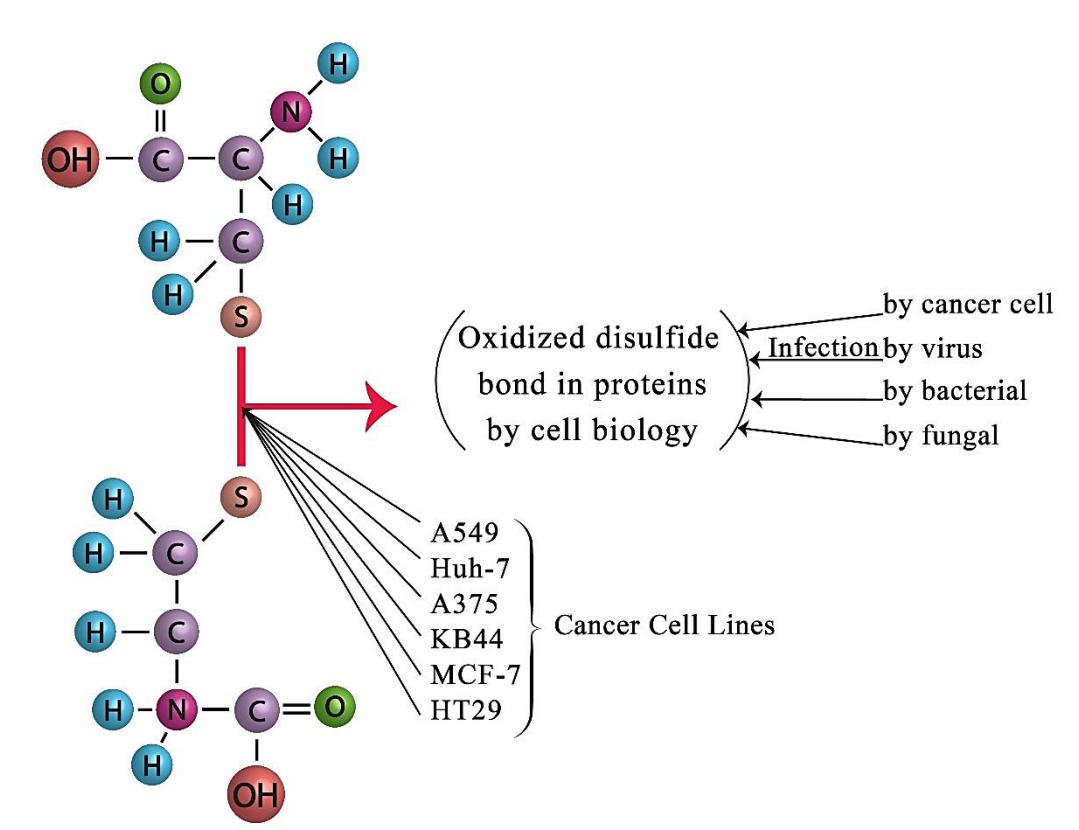

Fig. 14. Representation of breaking of S-S disulfide bonds by various fatal biological agents. Several types of cancer cell lines, virus, bacterial and fungal can attack to the disulfide bonds and disturb their covalent bonds in proteins' folding and poly peptides in DNA. The formation and breakage of bonds in disulfide structure require electron acceptors and donor's reagents during the oxidation-reduction process.

Conclusions

In this present research in nanomedicine field, it was attempted to fabricate and formulate a unique and unrivaled nanodrug (nanopackage fluid product) for 6 various types of cancer cells. Author applied a network of selected semiconductors (ZnO and SiO_2 NPs) and fruitful (CNTs and Al_2O_3) NPs due to their unique properties in nano regime against cancerous cells. The major and basic of its components are: ZnO Q-Dot NPs, ZnO NPs@modified-CNTs, Al_2O_3@ Silica nanocomposites which dissolved in green pharmaceutical binder, suitable dispersant / viscosity control, nonionic surfactant as a special emulsifier, healthy polar solvent /distiller water solution in desirable pH value (7.40) for human body. It is interesting point that, the synthesize of ZnO NPs inside the hollow CNTs structure also makes them reasonable options for modern drug delivery, particularly slow drug release applications. All these nanomaterials along with activator reagents (such as ZnO, Al_2O_3 NPs and –COOH function) would fabricate our nanopackage fluid product. The interesting obtained achievements indicated the IC50 (µg/ml) values within 24 and 48 h for human lung carcinoma as 60, human Liver Cancer Cells as 75, human melanoma cells, skin cancer as 90, human nasopharynx carcinoma cell line as 65, human breast cancer cell line as 50, and human colon adenocarcinoma cell line as 75 µg/ml, respectively, whereas human Foreskin Fibroblast (HFF-2) was applied as a normal cell line (195 µg/ml). Such nanopackage was characterized by SEM, XRD, FTIR, photoluminescence (PL), UV–Vis blue shift spectroscopy. From these data, it was clear that, some of these NPs were very fine and small nanosized. Furthermore, they could diffuse through cell membrane and formed strong hydrogen bonds with amino acids of proteins at interface, producing reactive ROS, which generates special vital oxidation-reduction chemical reactions and in following binds the broken R-S-H° radicals to R-S-S-R (disulfide bridges) in DNA-protein crosslinks. This could be a prominent guide and a very attractive idea to make specific NPs or nanofluids for human virus infections (HIV, SARS, MERS, and COVID-19), as well. Because, the source of many cancer diseases are fetal viruses, so their performance of mechanism can be the same. It should be noted that, smart NPs do not let the virus or bacteria to break the vital bonds (-S-S-) in protein folding structures. Because, the splitting of S-S bonds usually leads to destruction of the unique three-dimensional structure of a protein macromolecule, which causes damaging immune system and loss of its biological activity (like HIV/AIDS infection). Overall, authors thought that some of these mechanisms which are generated by pernicious virus, bacteria and cancer cells, could behave similarly. Herein, robust and very fine NPs which have capability to respond to more than one biology systems such as types of virus/ bacteria/ fungi/and cancer cell lines, truly represent one of the most fascinating and unique benefits of nanotechnology in medicine.

Acknowledgments

The authors have the honor to thank and appreciate dr. Rouhollah Vahabpour for many helps to perform MTT assays and professor Azizollah Shafiekhani for unique advices on new physics topics. We are very grateful to prof. Mehdi Assmar for significant aiding in the virus and bacteria issues being related to cancer. Also, we are so thankful to Mrs. Sara Habibi for wonderful designing the schematic representation of chemical reactions in the nanopackage. Furthermore, we would like to express our deep gratitude to *Nanomedicine & Nanodrugs ZPH* company for the great valuable contribution on development of nanoparticles' smart surface design.

Disclosure statement

The authors report no potential conflicts of interest and are responsible for the content and writing of the manuscript.

References

1. R. Mahato, W. Tai, K. Cheng, Prodrugs for improving tumor targetability and efficiency, Adv. Drug Deliv. Rev., 63 (2011) 659–670.
2. S.S. Feng, Chemotherapeutic engineering: concept, feasibility, safety and prospect—a tribute to Shu Chien's 80th birthday, Cell. Mol. Bioeng., 4 (2011) 708–716.
3. R. L. Siegel, K.D. Miller, S.A. Fedewa, D.J. Ahnen, R.G.S. Meester, A. Barzi, A. Jemal, Colorectal cancer statistics, 2017, CA Cancer J Clin, 67 (2017) 177–193.
4. S.S. Lucky, K.C. Soo, Y. Zhang, Nanoparticles in Photodynamic Therapy, Chem. Rev., 115 (2015) 1990–2042.
5. W. Fan, B. Yung, P. Huang, X. Chen, Nanotechnology for Multimodal Synergistic Cancer Therapy, Chem. Rev., 117 (2017) 13566–13638.
6. L. Cheng, C. Wang, L. Feng, K. Yang, Z. Liu, Functional Nanomaterials for Phototherapies of Cancer, Chem. Rev., 114 (2014) 10869–10939.
7. J. Zhou, G. Yu, F. Huang, Supramolecular Chemotherapy Based on Host-Guest Molecular Recognition: A Novel Strategy in the Battle Against Cancer with a Bright Future, Chem. Soc. Rev., 46 (2017) 7021–7053.
8. S. Tran, P.J. DeGiovanni, B. Piel, P. Rai, Cancer nanomedicine: a review of recent success in drug delivery, Tran et al. Clin Trans Med, 6 (2017) 1–21.
9. X. Li, J. Kim, J. Yoon, X. Chen, Cancer-Associated, Stimuli-Driven, Turn on Theranostics for Multimodality Imaging and Therapy, Adv. Mater, 29 (2017) 1606857–1606880.
10. T. Sun, Y. S. Zhang, B. Pang, D. C. Hyun, M. Yang, Y. Xia, Engineered Nanoparticles for Drug Delivery in Cancer Therapy, Nanomed., 53 (2014) 1-46.
11. A.G. Cheetham, R.W. Chakroun, W. Ma, H. Cui, Self-Assembling Prodrugs, Chem. Soc. Rev., 46 (2017) 6638–6663.
12. D. Hanahan, R.A. Weinberg, The Hallmarks of Cancer, Cell, 100 (2000) 57–70.
13. R. Mrowczynski, Polydopamine-Based Multifunctional (Nano) materials for Cancer Therapy, ACS Appl. Mater. Interfaces, 10 (2018) 7541–7561.
14. Y. Yuan, T. Cai, X. Xia, R. Zhang, P. Chiba, Y. Cai, Nanoparticle Delivery of Anticancer Drugs Overcomes Multidrug Resistance in Breast Cancer, Drug Delivery, 23 (2016) 3350–3357.
15. X. Dong, R.J. Mumper, Nanomedicinal Strategies to Treat Multidrug-Resistant Tumors: Current Progress, Nanomedicine, 5 (2010) 597–615.
16. A. Wicki, D. Witzigmann, V. Balasubramanian, J. Huwyler, Nanomedicine in cancer therapy: challenges, opportunities, and clinical applications, J Control Release, 200 (2015) 138–157.
17. R. Sinha, G. J. Kim, S. Nie, D.M. Shin, Nanotechnology in cancer therapeutics: bioconjugated nanoparticles for drug delivery, Mol Cancer Ther, 5 (2006) 1909–1917.
18. G. Bisht, S. Rayamajhi, ZnO Nanoparticles: A Promising Anticancer Agent, Nanobiomed., 3, (2016) 1-11.
19. Z. Fakhroueian, A. M. Dehshiri, F. Katouzian, P. Esmaeilzadeh, In vitro cytotoxic effects of modified zinc oxide quantum dots on breast cancer cell lines (MCF7), colon cancer cell lines (HT29) and various fungi, J. Nanopart. Res., 16: 2483, (2014),1-14. DOI 10.1007/s11051-014-2483-2.
20. Z. Fakhroueian, R. Vahabpour, M. Assmar, A. Massiha, A. Zahedi, P. Esmaeilzadeh, F. Katouzian, S. Rezaei, P. Keyhanvar, A. M. Dehshiri, ZnO Q-dots as a potent therapeutic nanomedicine for in vitro cytotoxicity evaluation of mouth KB44, breast MCF7, colon HT29 and HeLa cancer cell lines, mouse ear swelling tests in vivo and its side effects using the animal model, Artificial Cells, Nanomedicine, and Biotechnology, (2018), 1-17. http://www.tandfonline.com/loi/ianb20

21. V.D. Subramaniam, M. Ramachndran, F. Marotta, A. Banerjee, X. F. Sun, S. Pathak, Comparative study on anti-proliferative potentials of zinc oxide and aluminum oxide nanoparticles in colon cancer cells, Acta Biomed., 90 (2019) 241–247.
22. J.W. Rasmussen, E. Martinez, P. Louka, D.G. Wingett, Zinc Oxide Nanoparticles for Selective Destruction of Tumor Cells and Potential for Drug Delivery Applications, Expert Opin Drug Deliv., 7 (2010) 1063–1077.
23. Z. Fakhroueian, F. Katouzian, Pegah. Esmaeilzadeh, S.M. Bidhendi, Pouriya. Esmaeilzadeh, Enhanced engineered ZnO nanostructures and their antibacterial activity against urinary, gastrointestinal, respiratory and dermal genital infections, Appl. Nanosci., 9 (2019) 1759–1773.
24. L. Nie, L. Gao, P. Feng, J Zhang, X. Fu, Y. Liu, X. Yan, T. Wang, Three-dimensional functionalized tetrapod-like ZnO nanostructures for plasmid DNA delivery. Small, 2 (2006) 621–625.
25. L.B. Naves, C. Dhand, J. R. Venugopal, L. Rajamani, S. Ramakrishna, L. Almeida, Nanotechnology for the treatment of melanoma skin cancer, Prog Biomater., 6, (2017), 13–26.
26. A. Vyas, S. K. Das, D. Singh, A. Sonker, B. Gidwani, V. Jain, M. Singh, Recent Nanoparticulate Approaches of Drug Delivery for Skin Cancer, Trends in Appl. Sci. Res., 7, (2012), 620-635.
27. P. Hassanpour, Y. Panahi, A. Ebrahimi-Kalan, A. Akbarzadeh, S. Davaran, A. N. Nasibova, R. Khalilov, T. Kavetskyy, Biomedical applications of aluminium oxide nanoparticles, Micro & Nano Letters, 13 (2018) 1227–1231.
28. S. Jafari, H. Derakhshankhaha, L. Alaei, A. Fattahi, B. Shiri Varnamkhasti, A.A. Saboury, Mesoporous silica nanoparticles for therapeutic/diagnostic applications, Biomed. Pharmaco., 109 (2019) 1100-1111.
29. W. Arap, R. Pasqualini, M. Montalti, L. Petrizza, L. Prodi, E. Rampazzo, N. Zaccheroni, S. Marchiò, Luminescent Silica Nanoparticles for cancer diagnosis, Curr. Med. Chem., 20, (2013) 2195–2211.
30. Q. Wang, P. Zhang, Z. Li, X. Feng, C. Lv, H. Zhang, H. Xiao, J. Ding, X. Chen, Evaluation of Polymer Nanoformulations in Hepatoma Therapy by Established Rodent Models, Theranostics, 9, (2019), 1426–1452.
31. S-B. Wang, Y-Y. Ma, X-Y. Chen, Y-Y. Zhao, X-Z. Mou, Ceramide-Graphene Oxide Nanoparticles Enhance Cytotoxicity and Decrease HCC Xenograft Development: A Novel Approach for Targeted Cancer Therapy, Front. Pharmacol., 10 (2019), doi: 10.3389/fphar.2019.00069
32. J. Chou, Y-C. Lin, J. Kim, L. You, Z. Xu, B. He, D.M. Jablons, Nasopharyngeal Carcinoma-Review of the molecular mechanisms of Tumorigenesis, Head Neck, 30, (2008), , 946–963.
33. A. Yousefi, A. Safaroghli-Azar, Z. Fakhroueian, D. Bashash, ZnO/CNT@Fe3O4 induces ROS-mediated apoptosis in chronic myeloid leukemia (CML) cells: an emerging prospective for nanoparticles in leukemia treatment, Artificial Cells, Nanomedicine, and Biotechnology, 48, (2020), 735–745.
34. M.H. Abdolmohammadi, F. Fallahian, Z. Fakhroueian, M. Kamalian, P. Keyhanvar, F.M. Harsini, A. Shafiekhani, Application of new ZnO nanoformulation and Ag/Fe/ZnO nanocomposites as water-based nanofluids to consider in vitro cytotoxic effects against MCF-7 breast cancer cells, Artificial Cells, Nanomedicine, and Biotechnology, 45, (2017), 1769-1777.
35. J. Jiang, J. Pi, J. Cai, The Advancing of Zinc Oxide Nanoparticles for Biomedical Applications, Bioinorg. Chem. Appl., 2018, (2018) 1-18.
36. C. Nieto, M.A. Vega, G. Marcelo, E.M. Martín del Valle, Polydopamine nanoparticles kill cancer cells, RSC Advances, 8, (2018), 36201-36208.
37. R. Nasr, H. Hasanzadeh, A. Khaleghian, A. Moshtaghian, A. Emadi, S. Moshfegh, Induction of Apoptosis and Inhibition of Invasion in Gastric Cancer Cells by Titanium Dioxide Nanoparticles, Oman Med J. 33 (2018) 111–117.
38. R. Khademolhosseini, A. Jafari1, S.M. Mousavi, M. Manteghian, Z. Fakhroueian, Synthesis of silica nanoparticles with different morphologies and their effects on enhanced oil recovery, Applied Nanoscience, 10 (2019) 1105–1114.
39. R. Nandanwar, P. Singh, F.Z. Haque, Synthesis and Characterization of SiO2 Nanoparticles by Sol-Gel Process and Its Degradation of Methylene Blue, American Chemical Science Journal, 5 (2015) 1-10.
40. A. Alessi, S. Agnello, G. Buscarino, F.M. Gelardi, Raman and IR investigation of silica nanoparticles structure, Journal of Non-Crystalline Solid, 2013, 362, 20-24.
41. P.A. Prashanth, R.S. Raveendra, R. Hari Krishna, S. Ananda, N.P. Bhagya, B.M. Nagabhushana, K. Lingaraju, H. Raja Naika, Synthesis, characterizations, antibacterial and photoluminescence studies of solution combustion-derived α-Al2O3nanoparticles, Journal of Asian Ceramic Societies, 2015, 3, 345–351.
42. B. Shirkavand Hadavand, K. Mahdavi Javid, M. Gharagozlou, Mechanical properties of multi-walled carbon nanotube/epoxy polysulfide nanocomposite, Materials and Design, 50 (2013), 62–67.
43. P. Rauwel, M. Salumaa, A. Aasna, A. Galeckas, E. Rauwel, A Review of the Synthesis and Photoluminescence Properties of Hybrid ZnO and Carbon Nanomaterials, J. Nanomater., 2016 (2016) 1–13.
44. R. Chandrakar, R.N. Baghel, V.K. Chandra, B.P. Chandra, Synthesis, characterization and photoluminescence studies of undoped ZnS nanoparticles, Superlattices and Microstructures, 84 (2015) 84 132–143.
45. S. Senapati, A. Mahanta, S. Kumar, P. Maiti, Controlled drug delivery vehicles for cancer treatment and their performance, Signal Transduction and Targeted Therapy, 3 (2018) 3 1-19.
46. F. Yanık, F. Vardar, Toxic Effects of Aluminum Oxide (Al2O3) Nanoparticles on Root Growth and Development in Triticum aestivum, Water Air Soil Pollut., 226 (2015), https://doi.org/10.1007/s11270-015-2566-4.
47. M. Miyazawa, T. Ishii, K. Yasuda, S. Noda, H. Onouchi, P.S. Hartman, N. Ishii, The Role of Mitochondrial Superoxide Anion (O2–) on Physiological Aging in C57BL/6J Mice, J. Radiat. Res., 50 (2009) 73–82.
48. C. Garrido, L. Galluzzi, M. Brunet, P.E. Puig, C. Didelot, G. Kroemer, Mechanisms of cytochrome c release from mitochondria, Cell Death and Differentiation, 13 (2006) 1423–1433.
49. L.B. Poole, The Basics of Thiols and Cysteines in Redox Biology and Chemistry, Free Radic. Biol. Med., 80 (2015) 148–157.
50. J. Zhang, H. Tang, Z. Liu, B. Chen, Effects of major parameters of nanoparticles on their physical and chemical properties and recent application of nanodrug delivery system in targeted chemotherapy, Int J Nanomedicine, 12 (2017) 8483–8493.
51. Y. Yuan, T. Cai, X. Xia, R. Zhang, P. Chiba, Y. Cai, Nanoparticle delivery of anticancer drugs overcomes multidrug resistance in breast cancer, Drug Delivery, 23 (2016) 3350–3357.
52. H. Ghaffari, A. Tavakoli, A. Moradi, A. Tabarraei, F. Bokharaei Salim, M. Zahmatkeshan, M. Farahmand, D. Javanmard, S.J. Kiani, M. Esghaei, V. Pirhajati-Mahabadi, A. Ataei-Pirkooh, S.H. Monavari, Inhibition of H1N1 influenza virus infection by zinc oxide nanoparticles: another emerging application of nanomedicine, Journal of Biomedical Science, 26 (2019) 1-10.
53. M. J. Feige, I. Braakman, L M. Hendershot, Oxidative Folding of Proteins: Basic Principles, Cellular Regulation and Engineering, CHAPTER 1.1: Disulfide Bonds in Protein Folding and Stability, (2018),1-33. DOI: 10.1039/9781788013253-00001.